Fluoroscopic Technology from 1895 to 2019
Drivers: Physics and Physiology

Balter, Stephen
Columbia University, Departments of Radiology and Medicine, New York, NY, USA

Abstract: X-rays were first observed when they caused a phosphor to fluoresce in Roentgen's laboratory. In the early years, X-ray tubes and their associated power supplies were unstable and often dangerous to use due to X-rays, exposed high-voltage wiring, and ozone. The hazards were well known. Even so many early fluoroscopists lost their hands or lives. Nevertheless, by 1900, fluoroscopy became a routine medical tool. Medical radiography evolved as well but was slowed by long exposure times and the difficulties of early 20th century photographic processing. By the 1940s, the technology had reached the level at which the equipment required little attention, permitting the operators to focus almost exclusively on the medical tasks. Several key papers from this time period discuss noise effects, the effects of dark adaption on visual perception, the need for brighter images without excessive radiation, and begin to introduce cognitive factors into image diagnosis. The X-ray image intensifier (II) introduced into practice in the 1950s was a major step toward addressing these problems. The II also produced enough light to permit photographic and cine recordings of its output. The II itself achieved a factor of two improvement in quantum efficiency when the ZnCdS input screen was replaced by CsI in the mid-1970s. Parallel developments in video technology enabled the deployment of video viewing as a replacement for direct optical viewing. Photographic image subtraction was a key aspect of angiography. By 1980, analog and digital subtraction of angiographic images was a key factor in the growth of interventional radiology. Improvements in X-ray tube technology yielded greater outputs which facilitated spectral shaping of the X-ray beams to better match the absorption properties of Iodine. This step simultaneously reduced patient irradiation and improved the visibility of contrast filled vessels. The image intensifier itself began to be replaced by solid-state detectors (FP) around 2000. The most common variant used, and still uses a CsI input layer that is similar to that found in IIs. Thus, the dosimetric characteristics these FPs is similar to IIs. By 2010, the imaging hardware had become relatively stable. Improved real-time image processing has enabled better coupling of the information in the image to the observer's eye. This has yielded further improvements in image utility while simultaneously reducing patient irradiation. The next decade is likely to see further advances in this direction.

Keywords— Fluoroscopy, interventional radiology, patient dose, image quality, image processing

CONTENT

I. INTRODUCTION
II. EARLY DAYS (1895 – 1920)
III. DIRECT FLUOROSCOPIC SCREENS (1905-1960)
IV. THE OBSERVER'S EYE
V. RADIOGRAPHY BY PHOTOGRAPHY OF FLUOROSCOPIC SCREENS
VI. NOISE LIMITED IMAGING
VII. IMAGE INTENSIFIER WITH ANALOG IMAGE HANDLING (1955-1985)
VIII. ANALOG VIDEO (1960-2000)
IX. IMAGE INTENSIFIERS WITH DIGITAL IMAGE HANDLING and X-RAY BEAM SPECTRAL MANAGEMENT (1980-2000)
X. DIGITAL IMAGE PROCESSING (1980-2010)
XI. DIGITAL SUBTRACTION ANGIOGRAPHY (DSA) – (1980-2019)
XII. IMAGE PROCESSING, DISPLAY, AND STORAGE (1990 – 2010)
XIII. EXAMINATION CONFIGURATION
XIV. SOLID-STATE FLUOROSCOPIC IMAGE RECEPTORS (2000-2019)
XV. DIGITAL IMAGE PROCESSING (2010-2019)
XVI. COMMENT
XVII. REFERENCES
XVIII. ABOUT THE AUTHOR

I. INTRODUCTION

The evolution of fluoroscopic technology has driven by clinical requirements, technological possibilities, and the operational necessities of real-time imaging. Fluoroscopic procedures are used to monitor the motion of clinical objects using sequences of transitory images. Supplementary technologies are used to acquire and preserve a fraction of these images for later analysis. Most fluoroscopic procedures use real-time imaging while manipulating the patient, objects within the patient, and the imaging geometry needed to optimally view these objects. This process exposes the patient to radiation risks. Fluoroscopy frequently requires the presence of operators close to the patient and results in their exposure to radiation risks as well.

Fluoroscopy always requires that operators play a continuously active role while a procedure is in progress. The operator's physiological requirements, knowledge of the patient's condition, and immediate visual feedback provide key real-time operational inputs to the fluoroscope. This is fundamentally different than radiography, where images are usually acquired using a predefined protocol and there is seldom any interaction between physician and patient during clinical utilization of the images.

Key non-hardware concepts needed to understand the fluoroscopic environment include the physiology of human vision, the presence of a noise-defining quantum sink in the imaging chain, and the use of image processing to improve the conspicuity of clinically important structures. Many of the technological jumps that occurred in the past century are direct responses to requirements imposed by these concepts.

II. EARLY DAYS (1895 – 1920)

Roentgen's sequence of three original papers [1-3] and other early sources outline both similarities and difference between fluoroscopy and acquisition. For example: Roentgen's first observation was the fluorescence of Barium platinocyanide on a piece of cardboard when his Crookes tube was powered. It was reported that he saw a transient image of his own hand on the screen while manipulating an object with the beam on. The radiograph of his wife's hand was probably produced to document this observation.

Crookes tubes, their associated high-voltage sources, and other relevant items, were available in many physics laboratories around the world when Rontgen's discovery was announced in December of 1895. Experiments, including fluoroscopy, were reported around the world within weeks. Given the number of reports in the following few months, everything needed to produce fluoroscopic images must have been immediately at hand in many physics laboratories. Medical X-ray imaging ensued in many of these venues within weeks of the announcement. An anonymous research review was published in Nature in June 1896 [4]. It starts with: "The novelty of Prof. Rontgen's skeletal photographs has almost worn off, and the field of research opened up by his observations is now mainly occupied by scientific workers …" Nevertheless, there was continued physicist interest in X-ray imaging. Figures 1 and 2 document two anonymous nineteenth century setups with an induction-coil as the high-voltage source and a cryptoscope as the fluoroscopic detector. The tube in Figure 1 appears to be a basic Crook's design. The tubes in Figure 2 may already be contain an anode and a concave cathode. These features serve to increase X-Ray output and sharpen the image.

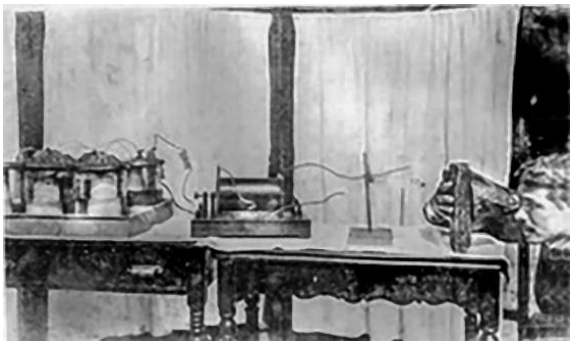

Fig 1: c 1896 Physicists' fluoroscope.

The monocular cryptoscope is the only item that may not have been immediately available in a typical physics lab following Roentgen's announcement in 1895. The investigator is using his own hand as a test-object. There were several published reports of hand injuries before the end of 1896. Source - ANON

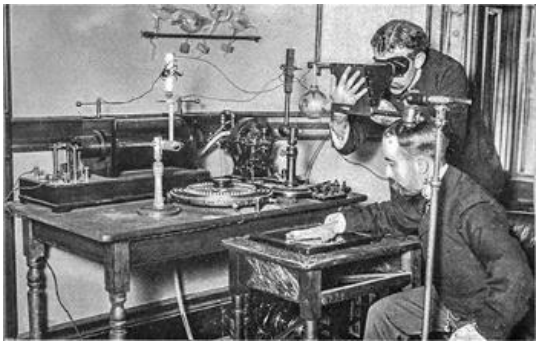

Fig 2: 1899 Radiography and Fluoroscopy.

This ubiquitous photo of a seated individual's hand is being radiographed while the standing individual is simultaneously using a cryptoscope to fluoroscope his own hand. This image could be either a posed picture or the fluoroscopist is using his hand as a QA tool while he adjusts the apparatus. . Note the supply of additional X-ray tubes on the far wall. Source – ANON

As shown in Figures 1 and 2, many early radiation workers used fluoroscopy with human hands as test objects with catastrophic consequences. Among other 1896 reports is an extended first-person description of major tissue reactions on the author's hands published in October [5].

X-rays outputs from gas-discharge tubes are unstable. Roentgen described a tool for describing imaging characteristics of the beam in his third paper [3]. It is simply a sheet of platinum with an array of holes. Each hole is covered with a different thickness of aluminum. The images of the tool provide the thickness of aluminum needed to match the transmission through the surrounding platinum. This tool is a variant of the Bunsen photometer used for measuring light intensities in the pre-electronic era. The underlying physics of atomic number dependent differential attenuation is the basis of many 20th and 21st century test tools. Many other fluoroscopic test objects, and reference objects for characterizing patient images were described in the literature before 1900.

Direct observation of the fluoroscopic screen involves directly converting a fraction of the energy carried by an X-ray beam into visible light (fluorescent-yield). Image visualization requires enough light to activate either the human visual system or a photographic plate. In the weeks after receiving the first news about Roentgen's discovery, Edison screened a vast number of compounds for their fluorescent-yield and reported calcium tungstate (CaW) as the optimum in 1896 [6]. Ba[Pt(CN)4] produces green fluorescent light, and CaW produces blue light. The dark-adapted human eye is more sensitive to green than blue. CaW became the phosphor of choice for radiographic intensifying screens. Fluoroscopic screens eventually used green-emitting zinc-cadmium-sulphide (ZnCdS) as the phosphor of choice. ZnCdS was also used as the input screen for the first few generations of image intensifiers, until it was replaced by CsI in the 1980s.

The same report [6] goes on to say "The importance of this [fluoroscopic] apparatus to the surgeon cannot be over-estimated. It will give him an instant diagnosis of his case. The photographic method involves long exposure, in itself an evil, followed by the slow development and drying of the plate, and, worst of all, the uncertainty of getting any result whatever. The fluoroscope tells the story at once." Edison was a very active investigator of X-rays from within weeks of Roentgen's announcement until his assistant Clarence Dally became the first fatality from radiation in 1904 [7]. Because of this, Edison totally stopped all work with X-rays with the following comment: "Don't talk to me about X-rays, I am afraid of them."

In the nineteenth century most X-ray imaging was fluoroscopy using a hooded enclosure or a hand-held open fluoroscopic screen as the image receptor. The hooded system is called a cryptoscope in this paper to distinguish this technology from other types of fluoroscopic systems.

Figures 3 and 4 1897 show fluoroscopy in use for customs inspections. These are from the same Scientific American article [8]. The photograph in Figure 3, indicates that the working environment was illuminated.

Fig 3: 1897 baggage inspection.

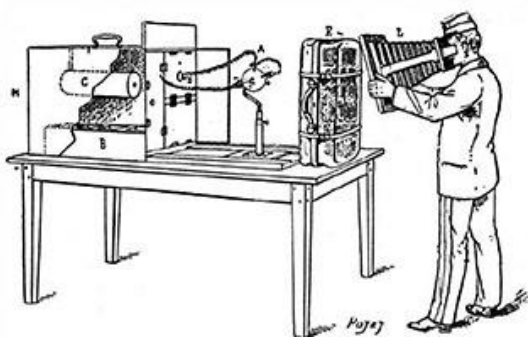

Source – Scientific American – Permission Pending

Figure 4 is a drawing of an open fluoroscopic screen used to search a woman for contraband in a darkened room. The X-ray components (box, tube, tube-stand) are identical to those in Figure 3. Photography in the dark was simply not possible in the 19th century. This image has also taken on its own life over the years; one version is captioned 'x-ray parlor games'

Fig 4: 1897 open fluoroscopic screen

Customs inspection detecting contraband. The woman on the right appears to be a badged customs officer. This image was included in the article cited in Figure 3. It has been reproduced many times with captions such as "X-ray parlor games".

Source – Scientific American – Permission Pending

Figure 5 contains a photograph of an early fluoroscopic examination. The source of this image is unknown but must be prior that of the almost identical French adverting postcard (Welcome Trust) The X-ray system seen in the images has essentially the same components as the system shown in Figure 1. The 19th century equivalent of photoshop must have been used to produce the 'original' photo on the left. The fluoroscopic image of the patient is far brighter than possible with direct fluoroscopy and two left elbows are seen (one on the screen) and one outside the boundary of the screen).

Fig 5: Pre 1900 Chest Fluoroscopy

a) Photograph with 19th century 'photoshop'. ANON

b) c 1898 advertising postcard. Source -Welcome Trust – permission pending

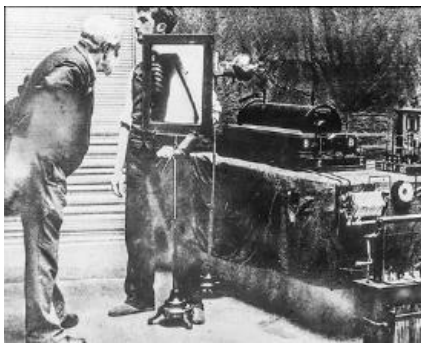

A

B

Fig 6: 1896 Complete X-ray system.

The unshielded X-ray tube is just right of center There is an attached spark-gap voltmeter mounted on the wall. The image receptor consists of a large fluoroscopic screen. A black cloth hood like the hood used photographic cameras of the era isolates the operator from room light. Source – Siemens Healthineers.

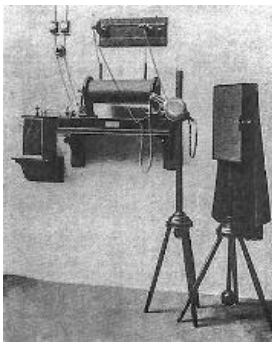

Complete X-ray sets were soon offered by major electrotechnical companies such as the Siemens set shown in (Fig 6). There were many other firms providing X-ray equipment and supplies c 1900. The surviving 1905 third edition catalog from Friedlander is fascinating. Beyond tubes, tube-stands, and generators this catalog provided instructions for battery-fluid film-processing chemistry, and assortment of radiation protection materials. Examples of radiation PPE are shown in Figure 7. The need for these devices was driven by reports of hand damage as early as 1896[9] and the death of Clarence Daily (Edison's assistant) in 1904[7].

Fig 7: Radiation Protection Devices

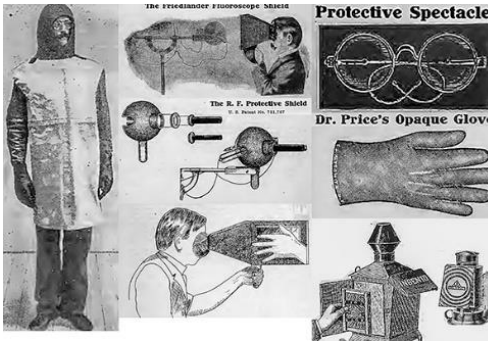

a) Selected offerings from 1905 Friedlander catalog No. 3. Source – Public Domain

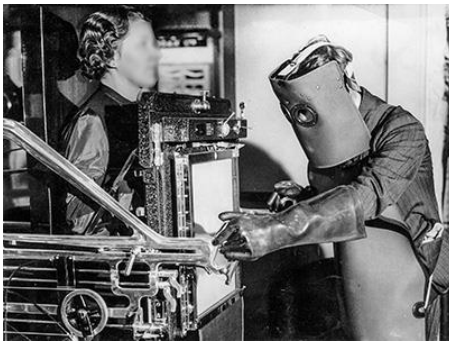

b) c 1940. What the well-dressed fluoroscopist might wear Source - ANON

Electrotherapy equipment was commercially manufactured and distributed in the late 19th and early 20th centuries. These devices used high-voltage sources that could produce X-rays in an increasing variety of gas-discharge tubes. By the turn of the century, McIntosh Battery & Optical Company a manufacturer of electrotherapy equipment, was able to supply commercial X-ray sets by adding a tube and cryptoscope to their existing product line. Fig 8 reproduces a 1915 advertisement from this company. Despite the image of an irradiated hand in the ad, this manufacturer was aware of the dangers of using the operator's hand as a QA tool. Commercial fluoroscopic QA tools have been around for more than a century. McIntosh offered a multi-target penetrometer with each target characterized as 'inches of flesh'. The long handle allowed the tool to be used without needing a hand in the beam. A similar penetrometer (without the handle) was offered in the 1905 Friedlander catalog.

Fig 8: 1915 Fluoroscopic set and an accessory QA tool

See text for the description.

Source - ORAU Health Physics Historical Museum – permission pending

Early in the gas-tube era, it was stated that radiography added no value to the fluoroscopic examination. There was likely to be partially true because that required long radiographic exposure times (typically tens of minutes) often resulted in motion blur. Photographic processing of radiographs was also in its infancy. Unfortunately, many early fluoroscopists were not content with brief observations; this resulted in many instances of radiation injury of both patients and operators. A decade or so later, better X-ray sources and improved radiographic receptors changed to advise that fluoroscopy should be only used for procedures requiring the observation of motion. Figure 9 reproduces two 1910 cryptoscopic head examinations[10]. Skull fluoroscopy was rare in this era. Figure 10, from the same textbook edition illustrates documentation using notes about or tracings of the fluoroscopic images. This textbook specifically advises that "radiography should be used for documentation instead of fluoroscopy whenever possible."

Fig 9: 1910 Textbook illustrations
The glass bowl supporting the gas X-ray tube is an electrical insulator. The X-ray tube in the left image is contained in a glass bowl that appears to have a partial lead shield similar to the shield offered in the Friedlander catalog (Fig 07). Note the exposed high-voltage wiring. The right image shows an unshielded X-ray tube. Source - Tousey 1910

Fig 10: 1910 Image documentation Captions in original advises to use radiography instead of notes or sketches based on fluoroscopy for documentation. Source - Tousey 1910

The need to have one or both hands free to manipulate the patient, adjust the X-ray controls, and document the imaging findings resulted in mechanical fluoroscopic screen holders attached to some form of patient support. The evolution of patient support mechanisms is a key part of fluoroscopy history from 1900-1950. The critical elements were anatomically positioning the patient for the procedure and giving the physician appropriate access to the patient during the procedure. Figure 11 illustrates two such systems. From the dates of the pictures, the X-ray sources were gas tubes. Along with radiation, exposed high voltage wires and ozone production were real dangers. These goals had to be met for procedures that were done in complete darkness. As time progressed systems incorporated improvements in both electrical and radiation protection for patients and staff.

Fig 11: Vertical Fluoroscopes

a) (1907) "the Kinescope allowed fluoroscopic examination and X-ray photography of patients standing, sitting, or lying with only one device." Source - Siemens Healthineers

b) Lead screen cover over the X-ray tube indicated in caption. Source – Tousey 1910

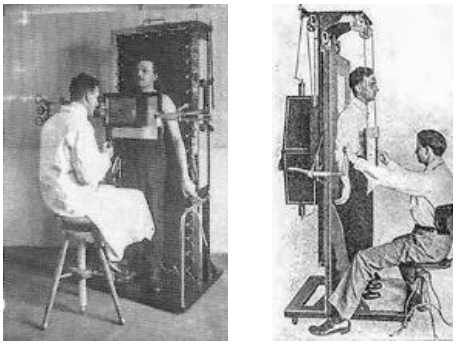

As shown in Figure 12, fluoroscopic guided surgery using a gas-tube and a head-mounted cryptoscope was in use for fluoroscopically guided surgery in WW-I. This is an early example of a fluoroscopically guided interventional procedure. Cryptoscopes remained in military and civilian use through the 1940s for both medical and non-medical purposes.

Fig 12: Military cryptoscopes

circa 1916

1944 US Navy Art Collection

1944 Europe

III. DIRECT FLUOROSCOPIC SCREENS (1905-1960)

The gas-tube era ended in the later part of the 1010's when hot-filament X-ray tube and transformer driven power supplies replaced gas tubes and induction-coil/static-generator high-voltage sources. The operational simplicity of these newer components helped transition daily use of radiography and fluoroscopy from a focus on equipment technology to a focus on radiation and imaging.

The transitions from gas-tubes and hand-held screens occurred in stages. Figure 13 is from Acme's 1926 advertisement for a horizontal table. The fluoroscopic screen is above the table. The poles on the left are tie-points for the high-voltage wiring. The radiographic tube holder (minus the tube itself-probably it was a hot-filament tube) is over the table with its fixed collimator. The tube is mounted in a lead-glass bowl which served both as a radiation barrier and an electrical insulator. The fluoroscopic tube is encased in a light-tight enclosure under the table. This enclosure may or may-not have had lead shielding. There is exposed high voltage wiring over and under the table. Nevertheless, this apparatus was used for fluoroscopy in a completely dark room.

A comparable 1940 Picker table is shown in Figure 14. Protection against electrical hazards with the introduction of flexible insulated high-voltage cables. The enclosed table contributed to reducing the amount of scatter reaching the operator. Equipment mounted specific radiation protection elements are missing.

Fig13: 1926 horizontal table

This Acme system includes an over-table radiographic tube (with collimator) and an under-table fluoroscopic tube. The radiographic tube itself and its wiring are not shown in this image. The two poles on the left-hand side are insulators. In use, exposed high-voltage wires ran from these points to the X-ray tubes. The enclosure for the under-table fluoroscopic tube may have been provided to minimize stray light during fluoroscopy.

Source - ACME advertisement in RADIOLOGY

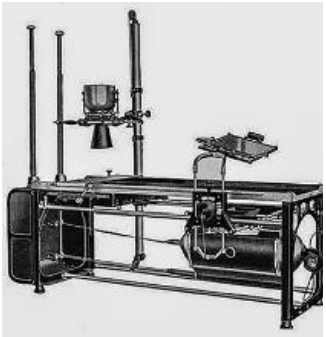

Fig 14: 1940 R/F table

Insulated high-voltage cables replace open wiring. The X-ray tubes used for such systems were typically shielded by lead contained within a grounded metal casing.

Source - PICKER advertisement in RADIOLOGY

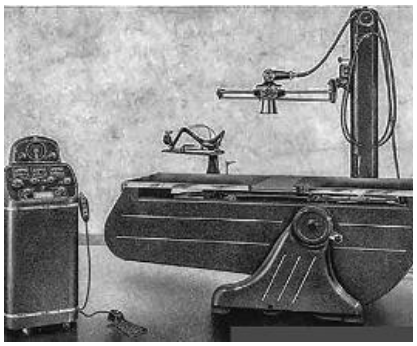

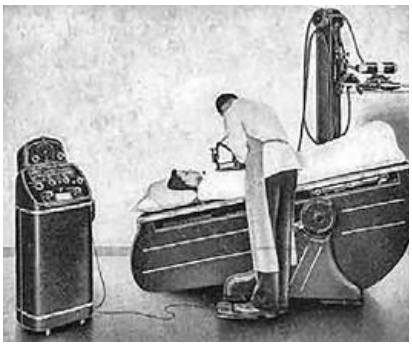

Figure 15 illustrates chest fluoroscopy in 1947. The original source of these images has been lost. Both appear to show the same fluoroscope. By this time, the fluoroscopic-screen may have had a lead-glass covering providing radiation protection to the operator. No collimation controls are immediately evident in either photo. If collimation was not available, the beam size would have been large enough to fully illuminate the screen in any position. The fluoroscopic screen is linked to the X-Ray tube assembly only in the vertical dimension. Thus, the vertical size of the beam need not have exceeded that of the screen. However, on the right-hand image, the screen is free to slide in the horizontal direction. This implies that the beam's horizontal size was substantially larger than that of the screen. This is undesirable. Eventually regulations required both collimation and a visible unirradiated margin on all four sides of the image. The heavy lead glove worn on the left-hand was used to palpate the patient under fluoroscopic control. It is also noted that the operator is not wearing any form of body radiation protection. There appears to be a lead apron draped over the chair back in the left-hand image. A portion of the scatter produced in the patient's chest could pass through the unshielded are between the bottom of the screen and the chair and thus irradiate the operator. Later standards specified a fully protected zone for the operator to manage irradiation.

Fig 15: 1947 Chest Fluoroscopy

See text for description

Source - ORAU Health Physics Historical Museum – permission pending

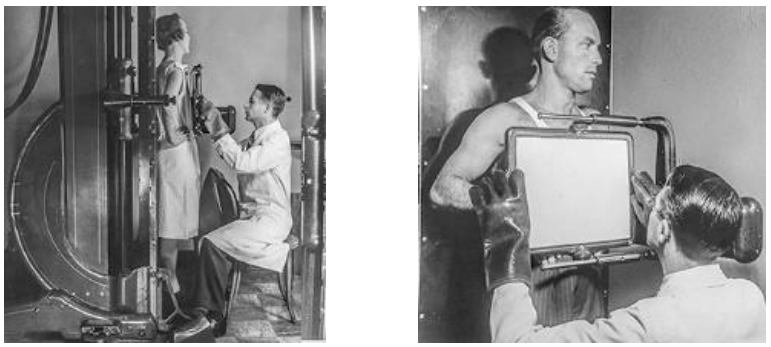

IV. THE OBSERVER'S EYE

The image on a fluoroscopic screen is only of value when it is transmitted to the observer's brain via the eyes. Aspects of vision intimately related to fluoroscopy are discussed in this section. The 10^{10} working light-intensity range of the human eye is needed to accommodate mid-day light levels in a cloudless desert and a subsequent moonless night(Fig 16). The anatomical basis providing this range includes two types of photoreceptors in the retina. The cone cells are activated by high light-intensity, the rod cells work at low light-intensity. Additional information is provided by standard vision and perception textbooks [11, 12].

Fig 16: Range of light intensities over which the human eye can accommodate

This range includes the effects of dark adaptation

Adapted from Chamberlain – 1942 [13]

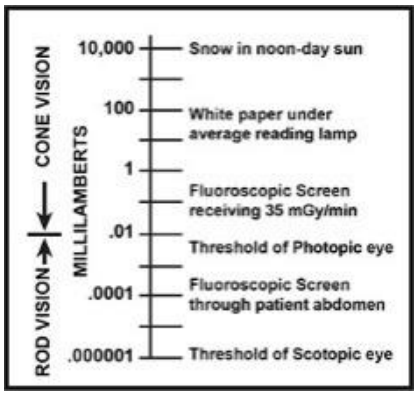

The increase in sensitivity of the eye to dim light is called dark adaptation. This process takes tens of minutes as shown in Figure 17. Note the break at the level where the cones have reached their maximum sensitivity, and the extension of sensitivity by several orders of magnitude where rod vision dominates.

Fig 17: Sketch of eye sensitivity as a function of dark-adaptation time.

The retina contains a mixture of visual cells called rods and cones. The cones are concentrated in the fovea, and rods compose the rest of the visual field.

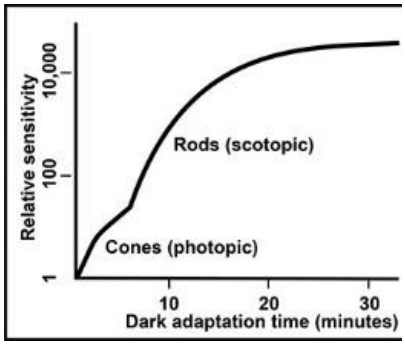

Figure 18 is from around 1955. Radiologists had to dark adapt for tens of minutes in order to optimally use their fluoroscopic screens. The radiologists are wearing red goggles which allows adaptation in typical ambient illumination. Radiographic film images could not be adequately read or interpreted while dark adapting. The goggles were removed after going into the fluoroscopic room and switching off the lights. There are many available photographs showing radiologists using their fluoroscopes while wearing red goggles. This is an impossibility because the screens emitted green light.

Fig 18: c 1955 dark adaptation with goggles.

Fluoroscopic screens could only produce a limited luminance at acceptable dose-rates. Operators dark adapted for about 30 minutes in order to fluoroscope at these low light levels. Typically, they wore red goggles and avoided bright lights during the adaptation time.

Source – ANON

Working with dark adapted eyes reduces the amount of radiation needed to form a perceivable image. Fortunately, the X-ray tubes available in the fluoroscopic-screen-era could not produce high dose-rates for long periods of time without sustaining irreversible thermal damage. Observers had to dark adapt in order to see anything of value. However, the costs of increased sensitivity include decreased spatial and temporal resolution of the visual system (Fig 19).

Fig 19: Sketches of spatial and temporal resolution at photopic and scotopic light levels.

Bright illumination levels enable foveal vision with the cones resulting in better spatial and temporal resolution. The present specification for minimum illuminance on diagnostic image monitors is intended to drive foveal vision.

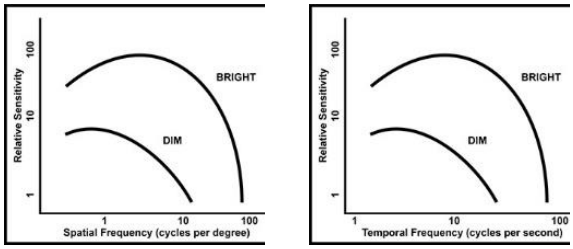

V. RADIOGRAPHY BY PHOTOGRAPHY OF FLUOROSCOPIC SCREENS

The concept of photographing a fluoroscopic screen was proposed before 1900. It was not practical then due to the limited light output of screens and the low sensitivity of early films. With better film and optics, photofluorographic systems, used for mass chest radiography were in common use from the 1930's through the 1960's [14]

Several of the surviving photographs (i.e. Fig. 10) indicate that sketching on top of the fluoroscopic screen and note-taking were in use. Several tools using direct irradiation of film-screen systems (spot-film-devices, kymography, 'rapid film changers') were used up to the 1980's but are mostly beyond the scope of this paper.

Rapid series imaging with a direct fluorescent screen was possible but not common. A 1950 system is shown in Figure 20. Based on the sample coronary angiogram, this system operated at several frames per second. The X-ray tube loading needed to sustain this framerate, and patient dose resulting from photographing direct screens, were too high to permit many frames, this inhibited general acceptance of this technology.

Fig 20: 1950 rapid sequence angiographic system

Uses a fluorescent screen and a photographic camera. This configuration was seldom used clinically. Along with limited image quality, patient radiation doses were almost certainly much higher than film-screen radiography.

Source - Siemens Healthineers

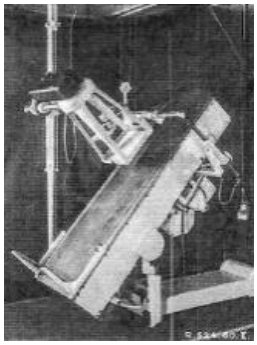

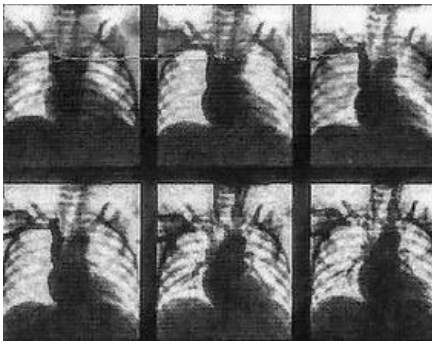

VI. NOISE LIMITED IMAGING

The perception of key clinical objects in an image is influenced by image noise. In a fluoroscopic image, visual noise can be grouped into two categories: The first is the noise produced by statistical variations in the numbers of X-Ray photons converted into light by the fluoroscopic screen (Quantum Noise). The second category is the combination of all other noise sources in the imaging chain and the observer's eye-brain system (System Noise). Quantum Noise is dependent on the local X-ray dose. System noise is independent of X-ray dose but may be dependent on factors such as illumination level. The amount of noise in an image changes with dose only when Quantum Noise is dominant.

For fluoroscopic-screens, quantum noise is significant if not totally dominant at patient entrance dose-rates of tens of milligray per minute. At any dose-rate. a device that amplifies illuminance of the observer's retina simply provides a brighter image without affecting quantum noise. Quantum noise is increased if the X-ray dose-rate is reduced. Low dose fluoroscopy may be far too (quantum) noisy for clinical use.

Higher dose-rates are required for direct fluoroscopy if the eye is not appropriately dark adapted. Under these circumstances, additional X-ray energy is needed to produce enough light for the observer to see. In broad terms, good screen-fluoroscopy was performed at dose-rates comparable to modern systems. Maximum dose rates were likely to have been physically restricted to a few hundred mGy/min by the construction of the X-ray tubes of the era.

Information flow through a fluoroscopic imaging system has been represented by a photon-flux-diagram since the 1940's [15]. Figure 21 introduces this model. The key concept is that radiographic and fluoroscopic images contain noise deriving from the quantum nature of the X-ray beam and modified at each step in the imaging chain. The ordinate is the number of photons per unit area. Several steps in the process are shown:

1) X-ray photon flux at the patient's skin (entrance exposure rate without scatter).
2) X-ray photon flux at the fluoroscopic screen (normalized to 1.0 for trajectories A and B)
3) Detected X-ray photons (25% of incident)
4) Light conversion (1,000 useful light photons per detected X-ray photon)
5) Useful light photons at the observer's eye (set to 2.5 for trajectories A,C and 0.25 for B)

The smallest number of signal carriers in a trajectory is called the quantum sink. In the quantum-limited trajectory (A), the number of visualized photons is an order of magnitude higher than detected X-Ray photons, indicating that X-ray quantum noise will dominate. The number of visualized photons in the poor-light management trajectory (B) is the quantum sink and is of concern. Since it is equal the number of detected photons on the same trajectory, it indicates that visualized noise will be higher than the native quantum noise. The equal light trajectory (C) delivers the same number of visualized photons as trajectory A, but at the cost of 10 X the patient input dose. Much of the technical development of image receptors in the subsequent half-century was focused on maintaining the quantum sink at the detected photon level instead of elsewhere in the imaging hardware.

Fig 21: Fluoro screen photon-flux diagram

A) QUANTUM LIMITED: The photon-flux density at the eye is 10 X the detected level. Entrance Exposure Rate (EER) = 50

B) POOR LIGHT MANAGEMENT: The photon-flux density at the eye is equal to that at detection stage. Visible noise is due to a combination of X-ray quantum noise and 'poor counting statistics' at the observer's eye. EER = 50.

C) EQUAL OBSERVER LIGHT (using the same ratio of emitted to visualized photons noted for B): Patient EER is increased by a factor of ten under these conditions EER = 500

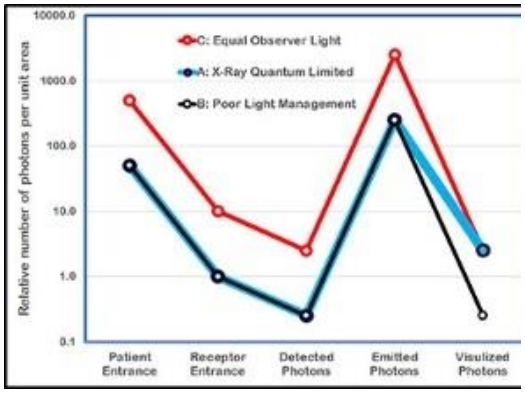

Sturm and Morgan's [15] original diagrams are reproduced in Figure 22. Patient entrance dose is constant for all three trajectories. Patient exit dose decreases for thicker beam projections. These change impact the downstream photon fluence density. The loss of flux inside the eye is an additional stage to those shown in Fig 21. This diagram indicates that the quantum sink is the observer's retina. The contrast-detail curves on the right are related to spatial sensitivity curve in Fig 19 with image noise as an additional driver. These experiments assumed a constant patient entrance exposure rate (left) Note the effect of increased image noise (due to lower output light flux) in trajectory C compared to trajectories A and B. In the right-hand drawing, the solid curves are experimental, and the dotted lines are corresponding theoretical predictions.

Fig 22: Effect of light level on contrast-detail measurements

Photon Densities in Fluoroscopy
(A – Chest; B – AP abdomen; C- LAT abdomen)
1 – Patient Entrance – identical for all three.
2 – Patient Exit
3 – Absorbed by Screen
4 – Light emitted by Screen
5 – Light entering Eye
6 – Absorbed by Retina

Source - Sturm & Morgan 1949[15] permission pending

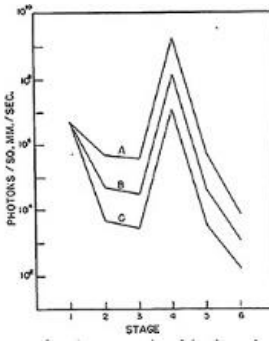

Photon Densities

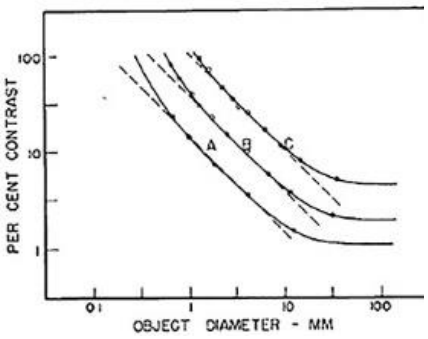

Corresponding Experimental Contrast-Detail Measurements,

VII. IMAGE INTENSIFIER WITH ANALOG IMAGE HANDLING (1955-1985)

Visibility of objects is influenced by brightness, contrast, object size, and visual noise. Chamberlain's 1942 Carman lecture [13] provided major insights into the influence of the human visual system on fluoroscopic imaging and introduced the first technical requirements for fluoroscopic image intensification. The enormous operating range of the human eye (Fig 16) is remarkable for any physical sensor. The eye's ability to discriminate differences is much lower when the rods are the active elements (low-level scotopic vision) compared to the cones (high light level photopic vision) (Fig 17,19). In 1948 Rose described the sensitivity of the human eye on an absolute scale [16] He summarized his finding as "The performance of the eye over the bulk of its operating range may be matched by an ideal picture pickup device having a storage time of 0.2 second and a quantum efficiency of 5 percent at low lights decreasing to 0.5 percent at high lights".

Chamberlain estimated that the brightness of a fluoroscopic image had to be increased by a factor of a thousand to enable photopic vision. This paper included a 1940 patent drawing from GE of an image intensifier (Fig 23). Several patent drawings from this time-period claim the image intensifier as a radiographic device instead of for use as a fluoroscopic tool.

Fig 23: 1940 Image Intensifier Patient Drawing

This patent drawing illustrates all the essential elements of an image intensifier except for minification (the output image is the same size as the input image.

Source - U.S. Patent 2,198,479

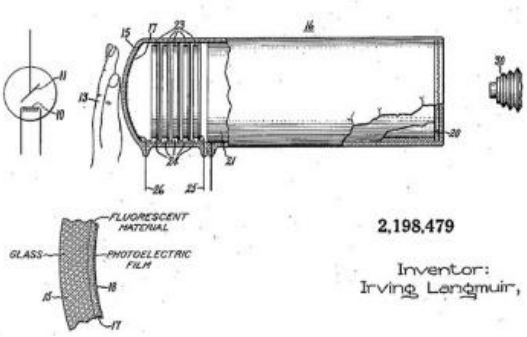

Coltman's 1948 paper 'Fluoroscopic Image Brightening by Electronic Means' [17] fuses the concepts of amplification and minification into what became the typical design of the fluoroscopic image intensifier. He also introduced a consideration of the effects of X-ray quantum limits on the perception of low-dose images. One important quote from this paper: "this is the fundamental limitation in image amplification, and that any system which does not make the fullest possible use of the available X-ray quanta incurs a deterioration of the image which cannot be corrected by subsequent amplification".

Figures 24 and 25 reproduces Coltman's electronic amplification only prototype device (perhaps based on a WW2 low-light goggle) and a sketch of an image intensifier tube with minification. Clinical X-ray intensifiers incorporate electro-optical minification (perhaps inspired by optical minification in photofluorographic chest systems), and electronic amplification. Image minification greatly improves the output light collection efficiency from such a tube. Figure 26 diagrams the conversion stages in an image intensifier tube that uses both electronic amplification and minification gain.

Fig 24: 1948 Prototype Image Intensifier

This device has electronic gain but does not utilize minification (input and output are the same size)

Source - Coltman 1948[17] – permission pending

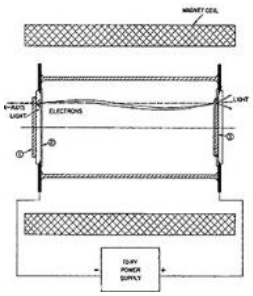

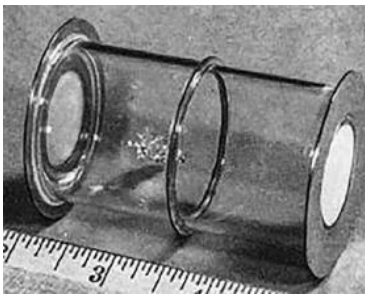

Fig 25: Image intensifier with minification

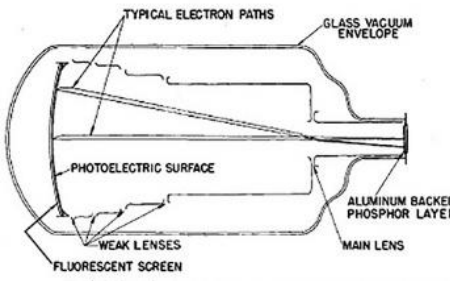

a) Schematic Source - Coltman 1948[17] – permission pending

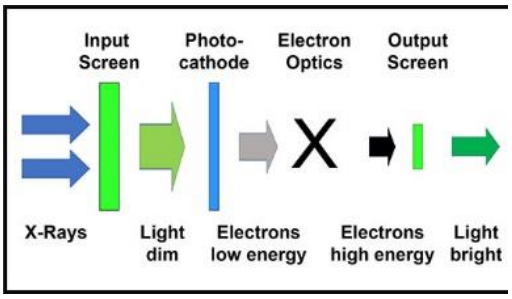

b) Conversion Stages

Image intensifiers produce a much brighter image than a fluoroscopic screen for the same X-ray input dose rate. In principle, the measurement is simply measuring the light output of a 'standard' fluoroscopic screen and the image intensifier under the same irradiation conditions. Practical problems include the definition of a 'standard' screen, and the performance of light meters in the 1960s. A standard based on the ratio of light out of the image intensifier divided by the X-ray input (Gx) was developed by the ICRU and published as NBS handbook 89 in 1963[18]. The measurement of Gx was reviewed in detail by Holm and Mosely in 1964[19]. This paper reports measurements on a single image intensifier and discusses the effects of X-ray spectral differences on the measurements and changes in Gx over time attributed to deterioration of the input layers of the tube.

Figure 26 schematically illustrates the measurement process and the effects of collimation and zoom on a tube's conversion factor. An X-ray beam having standard characteristics illuminates the tube's entrance. An ion chamber is used to

measure exposure-rate in the entrance plane and in the center of the field. A light meter measures light output (Cd/m^2) in the center of the output image. The Full FOV sketch indicates relative reference conditions. Neither measurement changes when the beam is collimated within the full FOV. However, the tube's minification gain diminishes when the tube is zoomed. More radiation is needed to produce the same light output. For an image intensifier: the radiation level scales with the ratio of the areas of the input and output screens (e.g. as the square of the ratio of input and output screen diameters). Looking ahead by four decades: In terms of radiation levels, zooming a flat-panel detector uses more or less of its input surface (similar to collimating an II). There is no need to adjust radiation levels with FOV because the brightness gain is independent of FOV. (Compensating for perceived noise as a function of FP zoom is discussed below.)

Fig 26: Image intensifier Conversion Factor
Gx = Light out / X-ray in. Gx is relative in this figure.

a) Max FOV – Low radiation to achieve light level: Gx = 10

b) Beam collimated within max FOV – Same radiation and light: Gx =10

c) Image intensifier zoomed – Higher dose rate needed to achieve the same light level: Gx-5

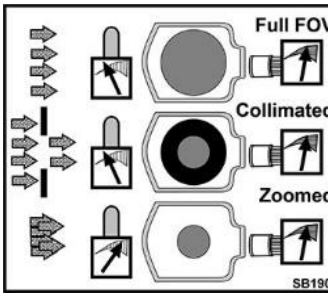

Coltman's assertion that amplification alone cannot be used to decrease irradiation is demonstrated with the use of a quantum flux diagram (Figure 27). This diagram adds an additional stage for light amplification to the stages in Fig 21. Trajectory A is for a fluoroscopic screen and is identical to the quantum limited trajectory in Figure 21 (amplification factor is 1.0). Trajectory B has the same input dose rate as A and a light amplification factor of 100, about enough to enable photopic vision. For trajectory C, the patient input dose rate is reduced by 100 to produce the same output light level as the screen (A). Now, the quantum sink is two orders of magnitude lower, producing an image that is too noisy for clinical use.

Fig 27: Image intensifier photon-flux diagram

See text

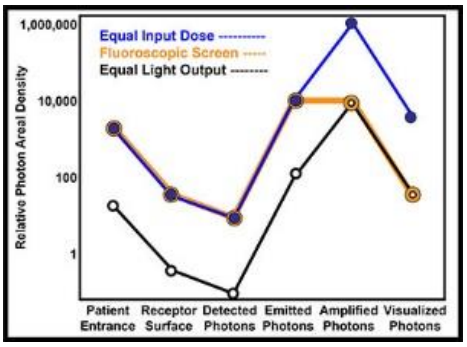

Coltman recommended constructing a system with a five-inch input screen based on considerations of clinical field-of-view, and bulk of the system. Its length was determined by electron-optics and scales with the size of the input screen. He stated: "The entire tube together with its housing, optical system, and protective lead shields, will be light enough to mount in place of the present fluoroscopic screen assembly on existing equipment". Figure 28 illustrates a different but representative 1955 single mode 5-inch tube.

Fig 28: c 1955 5" Image Intensifier

Note the optical relay lens which sent all available light from the II to the monocular viewing optic used by the system

Source - Philips Healthcare

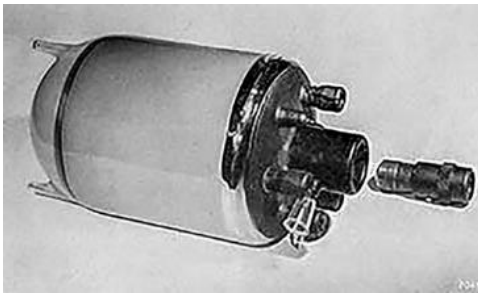

With image intensifiers, dark adaptation and dark fluoroscopic rooms were no longer required. Early image intensifiers had brightness gains of a few hundred times that of the brightness of the input screen. To permit operation at normal room

light levels, as many of the light photons produced at the output as possible had to reach the observer's retina. Monocular coupling was provided using optical periscopes. Figure 29 illustrates this in a 1956 Philips BV-20 mobile image intensifier with monocular viewing. A schematic drawing of the optical elements of this system is also shown.

Fig 29: 1956 Mobile Image Intensifier

a) Source - Philips Healthcare
b) Viewing - Photographed 2017
c) Monocular periscope output
d) Sketch of optics

Another variant of a single channel system is shown in Fig 30. Figure 30 illustrates a c 1955 table mounted gantry equipped with monocular viewing, a photographic camera that could be placed into the single viewing channel. The operator could not see the images while filming. Its optics are shown schematically for fluoroscopy and fluorography.

Fig 30: 1956 Cine image intensifier

a) single output channel for either monocular periscope fluoroscopy or cine-fluorography
Source - Philips Healthcare

b) Sketch of optics in fluoro and cine modes

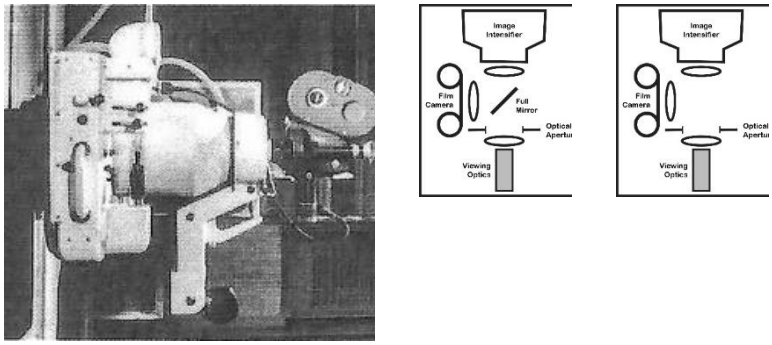

By the mid to late 1960s, direct fluoroscopic screens were increasingly replaced by image intensifiers. Figure 31 illustrates an image-intensified fluoroscope offered on the GE exhibit at the 1966 RSNA (my photo). The table includes a spot-film-tower mounted image intensifier. Looking at the right side of the photo, a direct fluoroscopic screen version was also offered for this system. Direct fluoroscopic screens remained in service throughout the world until their use was locally banned by local regulatory authorities. New direct screen fluoroscopic systems, including models with cryptoscopes, are still advertised on the internet. Direct screens may still be appropriate in regions where money is scarce and equipment service availability is low.

Fig 31: Transition

a) 1966 RSNA: System offered with either an image intensifier or a fluoroscopic screen

b) 2013 System with a fluoroscopic screen offered for sale on the internet.

In 1966 Morgan reviewed fluoroscopic imaging requirements in conjunction with the spatial and temporal performance of the observer's eye and available video technologies [20]. Figure 32 summarizes his findings for imaging a fixed object and a relatively high light level. This figure demonstrates both the effects of retinal physiology on the visibility of large or small objects and the influence of image noise (radiation dose) on minimum detectable contrast. The angle that an object subtends on the retina depends on both its size in the image and the observer's distance from the image. Higher dose levels are needed to suppress the noise conspicuity on more highly magnified images. A similar effect can occur when the large format viewing monitors found in many modern systems provides secondary image magnification.

Fig 32: 1966 Perception

"Threshold contrast plotted as a function of spatial frequency recorded on an observer's retina for three levels of noise contrast. Location of curves is shifted progressively upward as noise contrast increases."

Source- Morgan 66[20]– permission pending

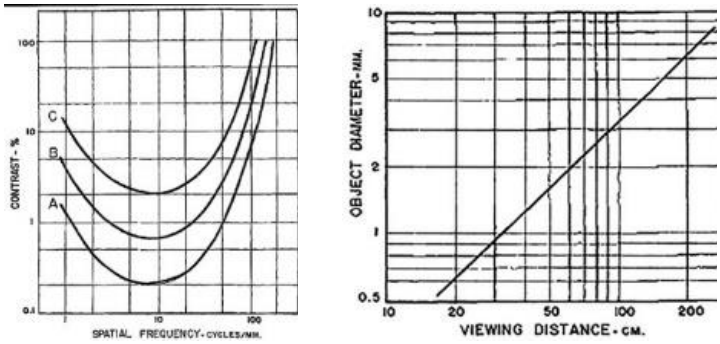

Improved image intensifier photocathodes increased the brightness gain into the few-thousand range. This yielded enough light to replace the periscope with mirror optics. Figure 33 illustrates two typical mirror-optic systems. Even though most of the light photons produced by the system did not enter the observer's eyes, there were enough photons on the retina to limit X-ray quantum noise to an acceptable level without the need for excessive patient dose. As predicted by Morgan [20], noise perception using systems with two or more fields-of-view, increasing magnification by selecting a smaller field-of-view required an increase in radiation dose for equal noise perception. This, along with the associated loss of minification gain in the image intensifier lead to dose-rate increases proportional to the ratio of the areas of the larger and smaller input FOVs. The interactions of radiation-dose and noise perception as a function of FOV remain important today for perceptual reasons.

Fig 33: Mirror Viewing

a) c 1960 Note backup direct fluoroscopic screen Source - Philips Healthcare

b) 1964 Note slot for spot-film cassette Source - PICKER advertisement in RADIOLOGY

c) Exit Pupil: Must be large enough to illuminate both of the observer's eyes. Most of the light from the II does not enter the eye.

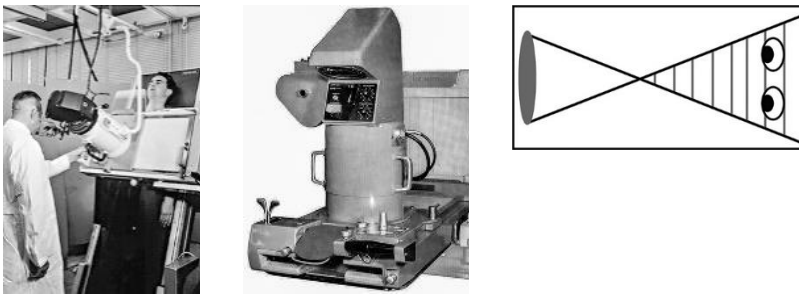

Collimating the X-ray beam to the clinical area of interest is an important radioprotetive measure for both patients and staff. Collimation also improves object visibility by reducing the scatter contribution to the image. The need for collimation was recognized by 1905 (Fig 7, 9), but often not provided (Fig 10,15) The introduction of small round image intensifiers posed a second issue (Fig 33). Collimators also had to irradiate the larger rectangular films used in spot-film devices. Rectangular collimators were supplied to meet filming requirements. There will be irradiated but not imaged areas in the patient when a square or rectangular collimator is used to fully illuminate the input of a round image intensifier.

Figure 34 shows Dr. F. Mason Sones performing diagnostic cardiac angiography using a 1956 11-inch image intensifier equipped with cinefluorography and periscopic viewing. The imaging system was too bulky to place over the patient. Thus, the imaging system, and operator, were in a pit below the patient table. A second individual handled the intravascular catheters without any ability to see the fluoroscopic images. This system has a beam splitter that permits viewing while filming. It also includes a phototube that measures the light intensity in a defined portion of the image (measuring field). A schematic of the optics of functionally similar later system is also shown. A later photograph of such a 'pit' lab includes an additional 5-inch over-table image intensifier with mirror viewing optics

Fig 34: Early Cardiac II

a) The 11" II was too bulky to operate above the patient.(1955).

b)1960 photo of a 'pit' lab shows a 5" over table II with mirror optics added to the setup .

c) Schematic sketch of optics

(a-c) Source - Philips Healthcare

d) corresponding optics sketch

A

B

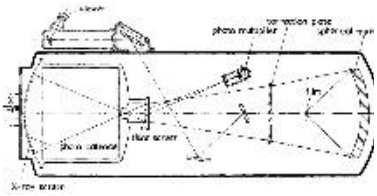

C

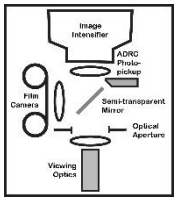

D

As noted above, this 11-inch device includes a photo pickup which indicates that the fluoroscopic system included an Automatic Brightness Control (ABC) circuit. Because such circuits work by controlling radiation output, the nomenclature changed to Automatic Dose Rate Control (ADRC). Photo pickups were incorporated into the optics used for most of the systems incorporating analog video chains. Further examples are shown in the sketches of image intensifier optics presented later in this paper.

Photo pickups measure the average light intensity in a defined area of the image intensifier's output image. X-ray factors are increased if the measured light level is too low and decreased if it is too high. The controlled elements were a combination of kVp, mA, and fluoroscopic pulse-width. The overall image became too bright if portions of the image in the measuring field included large amounts of contrast medium such as barium or iodine. Some systems provided a 'lock' option which allowed the operator to turn off the ADRC just before administering contrast. Investigators researching video densitometry in the 1970s and 1980s [21, 22] obtained unusual results if they did not understand the relationship between ADRC and contrast in the imaging field. Once images were digitized, ADRC control utilized analysis of appropriate areas of the digital image. Controls could now account for collimator size and position, as well as using examination specific measuring fields.

In many systems, the fluoroscopic ADRC sets system parameters for the next acquisition. If a different projection angle or body part is involved, it is a good idea to fluoroscope for a second before starting an acquisition.

Multi-mode (zoom) image intensifiers contain sets of internal electrodes which focus the photoelectrons collected from all or a portion of the photocathode onto a fixed output screen (Figure 35). This form of electronic magnification the system's required increase input radiation dose rates and could increase overall high-contrast resolution if the output-screen or other output elements are the resolution limiters. The minification gain of an image intensifier is proportional to the ratio of the areas of the input and output screens. To maintain constant brightness, the input dose rate increases inversely as the square of the diameter of the input screen.

Fig 35: c 1975

a) 9-inch dual field (6-9) image intensifier

b) Image intensifier factory
Vacuum pumping and outgassing stations are shown.

Source - Philips Healthcare

Analog video was introduced in the 1960s. This development removed a major limitation on the position of the operator relative to the patient (FIG 36). As a bonus, everyone in the room (including the patient) could see the fluoroscopic images It also enabled the development of remote-control fluoroscopes with the image intensifier under the table (Figure 37). Placing the image receptor under the table results in having the X-ray tube over the table. The irradiation of an operator's eyes is

potentially increased from backscatter from the X-ray beam's patient entrance port in this geometry. To minimize staff head irradiation, most modern fluoroscopic systems place the image receptor above the patient.

Fig 36: Video Fluoroscopy c 1975

a,b) Note both conventional film/screen and fluorographic acquisition devices
Source = Philips Healthcare
c) Sketch of optics with beam splitter for acquisition

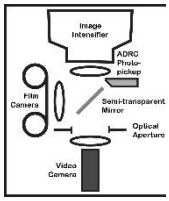

Fig 37: c 1978 Remote Control systems with under- table image intensifiers.

Increased above table scatter intensity may be a hazard.

a) Philips Healthcare
b) Siemens Healthineers
c) German Post Office

A

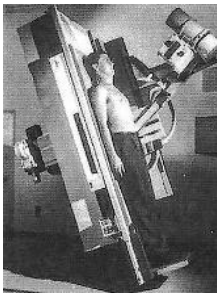

B

C

Fluoroscopic video systems usually used the broadcast video formats and standards of the countries where the systems were installed. The European standard was 25 frames per second with 625 lines per frame. The corresponding United States standard was 30 frames per second with 525 lines per frame. Both systems used 2:1 interlaced video to reduce image flicker. These values were selected to use and synchronize with the cycle rate of public power distribution systems (50 Hz in Europe; 60 Hz in the USA). Higher line densities and higher frame rates were well known in this era but only occasionally found in clinical systems.

The USA and European analog video systems were incompatible. Analog scan converters were developed to facilitate trans-border movement of broadcast video streams such as the Olympics. These devices essentially 'wrote' charge distributions representing the image onto a storage mesh while simultaneously the mesh was scanned using an electron beam in the other format. For visual reasons, neither did a single frame write saturate the mesh nor did a single frame read discharge the mesh. The analog scan converter tube was adapted as an image integration and storage element in both fluoroscopy and B-scan ultrasonic imaging. Analog scan-converters were eventually succeeded by digital counterparts. Digital-scan-converters are currently used for a variety of medical and non-medical applications. Image characteristics of video-based systems are discussed later in this paper.

Even early image intensifier systems provided enough light to expose photographic film using acceptable patient dose levels using doses per frame about ten times higher than fluoroscopy. To meet the greater image quality requirements in fluorography relative to fluoroscopy, this ratio is still broadly valid in the digital world of 2019. The image intensifier is the enabling technology for photo-fluorography (photographing single or slow sequences of images directly from the image intensifier) and cine-fluorography (photography at motion picture frame rates). Film-screen based spot-films continued in use for several decades for tasks such as gastrointestinal fluoroscopy. Cinefluorography (Cine) was rapidly adopted for imaging rapidly moving structures such as the heart. Figure 38 illustrates a 23 cm (9 inch) image intensifier equipped with a cine camera and back-up mirror optics. This system also has a television camera.

Fig 38: c 1970 Cine + video

Video and cine with a back-up mirror optic

Source – Philips Healthcare

Reliable analog video cameras suitable for routine hospital use were available by the late 1960s. These cameras eliminated the need for even back-up optical viewing. Video viewing became a major enabler of fluoroscopically guided angiography because video removed major constraints on the operator's position and posture. Figure 39 was taken in Dr. Sones' lab after video was introduced a few years later. The operator is now able to work at tableside to manage the patient and manipulate the angiographic catheter directly. Others in the room can also see the fluoroscopic images as they work. A similar c 1980 cardiac catheterization laboratory is shown on the right. The X-ray beam path is vertical both systems. Patients were rotated to achieve necessary clinical projections. Note the patient cradle in the 1980 laboratory.

Among other things, the use of video-fluorography[23] as a substitute for film placed in front of the image intensifier reopened the beam collimation question. An iris collimator that could provide a circular beam adjustable for both anatomic interest and the source-to-receptor distance (SID) is an ideal first step. Systems with rectangular collimators could be set up to fully irradiate the image intensifier (important for small FOVs), fully enclose the beam within the II's FOV, or provide some balance. Regulatory limits allowed necessary over-irradiation plus a small extra margin to accommodate mechanical tolerances. The latest draft equipment standards recognize that this is no longer necessary and will require the beam to be confined to within the active FOV.

Fig 39: Cardiac Video Viewing

X-ray system has a fixed vertical axis in both images.

Patient ls rotated for different clinical views in system b

Source - Philips Healthcare

Gantries with one and two degrees of rotational freedom were introduced in the 1970s (Figure 40). Moving gantries were safer for patents but needed new forms of staff scatter protection to replace that provided by fixed X-Ray tubes located in a shielded table base. Simultaneously optimizing patient safety, physician-patient access, and staff safety is still evolving. There is an extensive literature on this topic. A small subset is referenced in this paper [24-41].

Fig 40: Rotating X-ray gantries

Moving gantries introduced new concerns about operator irradiation

a) Scatter fields for system B

b) 1975 One rotational axis

Source - Philips Healthcare

c) 1995 Two rotational axis

Source - Siemens Healthineers

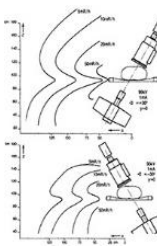

A

B

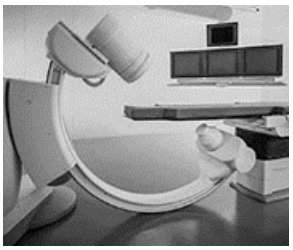

C

Most image intensifier assemblies used visible light to couple the output of the image intensifier tube to the observer's eye and/or cameras. Sketches of the optical handling systems (distributor) were shown in previous figures and continue in Figures 41 and 42.

Key elements in the distributor shown in Figures 41 and 42 include the photo pickup tube used by the ADRC, an optical diaphragm, and beam-splitters. In systems corresponding to Figure 40, the diaphragm was typically partially closed (degrading system brightness gain) to force enough X-ray flux to limit fluoroscopic X-ray quantum noise. Film cameras physically require more light than video cameras or the eye. The ADRC was programmed to accommodate that need resulting in less-noisy acquisition images. The beam-splitter diverted about 10% of the light into the viewing channel during photofluorography, allowing simultaneous viewing and image acquisition. The beam-splitter was removed during fluoroscopy, all available light was sent to the viewing channel, reducing X-ray dose rates to about 10% of photofluorographic levels.

Fig 41: Optical distributer with video and fluorographic cameras.

A 90%-10% beam splitter is used for fluorography which sends most of the light to the film-camera and passes enough to operate the video camera.

The beam splitter is mechanically removed for fluoroscopy to send all available light to video camera and thus minimize dose-rate.

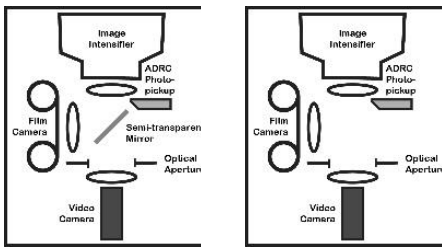

A - Cine **B - Fluoro**

The aperture had an additional function when photofluorography was replaced by video-fluorography (Figure 42). Closing the aperture for fluorography reduces the effective brightness gain of the system. This results in a higher x-ray dose rate for fluorography while maintaining a similar illumination level of the video chain for fluoroscopy and fluorography. Because the light level at the camera was similar for each mode, camera noise levels were similar.

Fig 42: Optical distributer with video-fluorography and optical ADRC

Optical aperture is closed for fluorography to minimize image noise. This requires an increased dose-rate for fluorography

Optical aperture is opened for fluoroscopy to minimize dose-rate

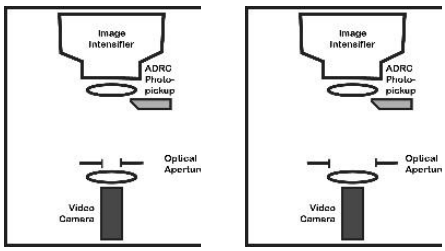

A - Cine **B - Fluoro**

The separate ADRC optical sensor was replaced by defining a ROI on the video images. The controlled optical aperture was retained for cameras with limited dynamic range. The aperture could be removed once wide dynamic cameras became available. Eventually the camera was placed in physical contact with the output of the image intensifier (Figure 43). X-ray and camera factors were set by selecting the operating mode of the system. In these configurations, camera noise is relatively higher for fluoroscopy than for video fluorography.

Fig 43: Optical distributer with video-fluorography and video ADRC

Optical aperture is opened for fluoroscopy to minimize dose-rate Optical aperture is closed for fluorography to minimize image noise. This requires an increased dose-rate

The entire optical system can be eliminated once video cameras with enough dynamic range became available. The dose-rate and pick-up camera operating conditions are set by selecting the fluoroscope's operating mode (fluoroscopy or acquisition).

Source - Philips Healthcare

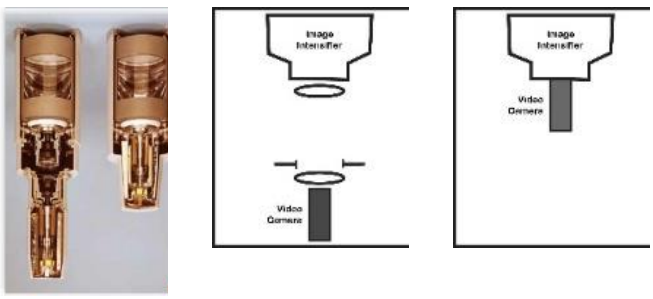

Film recording of image intensifier output images (fluorography) did not meet many non-cine clinical requirements until the 1970s. For example: Small FOV image intensifiers cannot image large anatomical structures without panning the imager. Direct film-screen systems (either spot-film devices or rapid film changers) were used and further developed in the 1960s.

Figure 44 illustrates typical film changers used for angiography. The fluoroscopic tube and its image intensifier were often separate assembly. Once the angiographic catheter was placed, the region of interest was moved to the film-changer zone (in some systems, the film-changer mechanically replaced the image-intensifier. Film-changers had maximum frame rates of 6 per second, and very limited film capacity (approx. 10 – 50 images). To complete a study with limited image capability, film-changers included control elements that varied framerates during a single angiographic run. Typically, there was a programmable time delay from the start of contrast-media injection until the first images; relatively rapid imaging during the arterial phase of the study (2-4 images per second) and slower imaging (approx. 1 image per second) during the wash-out and venous phases. Programmable frame timing saves radiation as well as film. Variable acquisition frame rates are still available on many c 2010 – 2020 digital angiographic systems. They are a valuable radiation management tool.

Fig 44: rapid film changer and controller

a) The AP changer is under the table at the left, the lateral changer is away from the table. The image intensifier is in the center. Separate X-ray tubes are used with each. Source - 1974 St. Vincent Hospital, Worcester MA

b) Sanchez-Perez cassette changer control module. Capable of programming variable frame rates during a single acquisition run. Source – Radiology Advertisement 1964

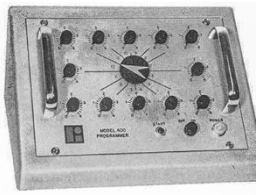

Until the mid-1970s, image intensifiers used the same ZnCdS phosphor for the X-ray detection as did the direct fluoroscopic screen. ZnCdS was deployed as small crystals dispersed in a binder (Figure 45). A fluoroscopic screen's efficiency in converting X-rays into visible light is proportional to the fraction of X-ray photons absorbed with active crystals (stopping fraction) and the crystal's ability to convert X-ray energy into visible light (conversion factor). Increasing the stopping fraction of a screen is accomplished by increasing the thickness of the screen. Thicker screens give light photons more room to scatter before they encounter the detector layer (the photocathode in the case of an image intensifier). Light scatter decreases image sharpness. The best image intensifiers had a stopping power of about 1/3. Patient dose rates were not very different for these two technologies under optimum conditions.

The introduction of CsI as a replacement input phosphor simultaneously reduced dose requirements by about a factor of two because of the higher X-ray stopping power of CsI, greater packing density of the active phosphor and reduced optical scattering in the screen because its structure is composed of crystals acting as light pipes. Figure 45 illustrates the differences between these two screens.

Fig 45: CsI Input Screen	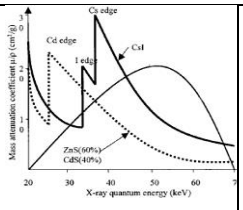	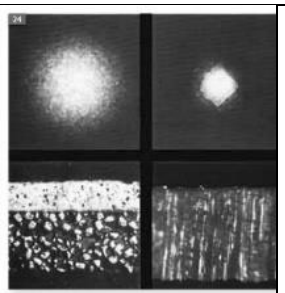	
	A - Physics	**B** - Comparison of ZnCdS & CsI Source-Philips Healthcare	**C** – Machlett Advertisement in Radiology

VIII. ANALOG VIDEO (1960-2000)

Every available analog video-camera technology was employed at some time in fluoroscopic systems (Fig. 46). Major species included the image-orthicon and the vidicon. Orthicons were the usual broadcast-television pick-up tubes of the 1860S. Broadcast video standards were developed around the orthicon's bandwidth and characteristically minimum signal integration at the detector which minimized motion blur of live video. The image tubes themselves, along with the array of analog vacuum tubes in the camera were bulky and required a great deal of ongoing maintenance. The vidicon provided

similar video outputs in a smaller package at the expense of increased image integration at the detector. The plumbicon is a form of vidicon, using lead-oxide in its detector, which exhibited less lag.

Fig 46: Video Tubes and cameras

a) Analog video tubes ranging from a 4" diameter orthicon to a ½" consumer vidicon

b) Orthicon broadcast camera Source – BBC

c) Orthicon Medical Camera Source Westinghouse ad in RADIOLOGY

A

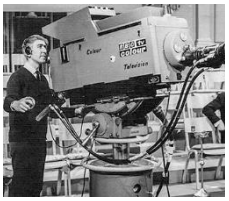

B

C

Lag in a video tube provided a benefit for fluoroscopic imaging before the era of digital video image processing. When the lag was not excessive, the tube effectively temporally averaged X-ray quantum noise producing a smoother image. Surviving anecdotes from that era include the report that orthicons were tested for lag before installation in broadcast cameras. Some of these broadcast rejects provided better fluoroscopic visual performance than the accepted tubes because of noise integration. X-ray manufacturers were reported to advertise these tubes as 'selected for medical use'. I was personally involved in the installation of a fluoroscopic system for GI examinations featuring the "new" low-lag plumbicon. The radiologists using this system were quite upset at the visual noise in the images. Because this was before the era of real-time image processing, the plumbicon was replaced with a higher image-lag vidicon to meet the radiologist's clinical requirements. Today, digital fluoroscopes artificially reproduce camera-lag using recursive filtering in their image processing software.

Analog broadcast video was transmitted using interlaced scans as a means of increasing the frame rate while constraining bandwidth. This is beneficial because the increased rate decreases the impression of flicker. Commercial motion pictures achieved the same result by projecting the same frame twice before advancing the film. Video interlacing results in a time lag between the two fields comprising a video frame (e.g. 1/60 of a second for 30 fps). Some anatomical structures (e.g. right coronary artery at systole) move fast enough to cause the structure's image to double. High frame rate, high bandwidth, non-interlaced video systems were available. While they performed well, the lack of standardization along with limited compatible third-party hardware, made image transport extremely difficult.

Analog video sequences can be recorded using either analog videotape or analog video disk. Maintaining image quality on these devices was very labor intensive. By the late 1970s, analog to digital scan-converters were able to extract either a single digital image or a sequence of digital images. These images were then locally stored digitally for processing and/or viewing. The availability of electronic images provided the technical infrastructure needed for digital angiography and digital subtraction angiography. The technical resources (networks, media, and displays) needed for digital archives were not available in that era. Digital fluorographic images were recorded on film for archiving using external laser or CRT based cameras.

IX. IMAGE INTENSIFIERS WITH DIGITAL IMAGE HANDLING and X-RAY BEAM SPECTRAL MANAGEMENT (1980-2000)

Fluoroscopic image outputs moved from pure analog imaging chains to hybrids with a single digital output for both fluoroscopy and fluorography in the 1980s. This was initially accomplished by processing the analog video signal using an analog to digital converter. Eventually a CCD camera replaced the analog video pickup tube. Hardware limitations early in this era constrained the output digital images to a nominal 512 x 512 pixel matrix with a maximum depth of 8 bits. Such images are adequate if detail averaging in a single pixel is not excessive and the intensity range in the entire image is accommodated within the available bit depth. Analog video – converter box systems were replaced by digital cameras (e.g. an array of digital sensor elements) with similar specifications. Technological advanced allowed greater matrix sizes and bit depts., while maintaining frame rates exceeding 30 fps.

By 1990, imaging chain design had reached the point where X-ray quantum noise was the major noise source for fluoroscopy. There was less than a factor of two available for reducing patient irradiation by improving the image intensifier. Radiation levels can be further reduced if radiological conspicuity of clinically important items, such as contrast media and guide wires, could be increased.

One way of improving the conspicuity of higher Z elements is to maximize the fraction of X-Ray photons in the beam with energies slightly above the K absorption edge of the material of interest. (e.g. iodine at 33.179 KeV). Filtering the beam by adding a layer of copper (0.1 – 1.0 mm) can accomplish this goal [42, 43]. Figure 47 is a sketch of the effect of this filter for a typical 70 KVp spectrum. Adding copper greatly reduces the fraction of the beam with energies below the iodine edge. It also decreases the total photon flux available to form the image. Increasing the operating voltage to 80 KVp does not help because most of the flux gain occurs at photon energies substantially higher than the iodine K edge. Reducing the KVP to 60

and increasing the tube current moves the photon spectral distribution closer to the Iodine K edge while simultaneously providing enough flux to meet imaging statistical requirements. This option became available in the 1990s when X-ray tubes were developed with enough long-time power ratings to meet this requirement without damage (Figure 48). The increased anode cooling in this class of tubes is partially attributable to the replacement of ball-bearing support for the anode assembly with liquid bearings.

Fig 47 Beam spectral shaping

See text

Dotted line is Iodine attenuation

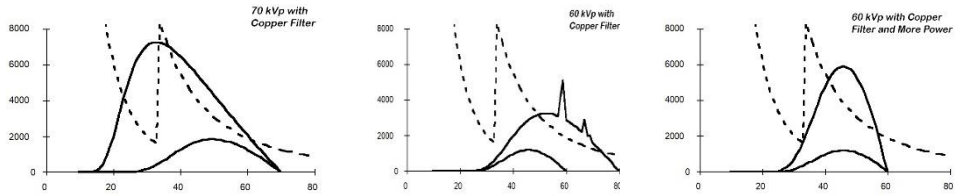

A – 70 kV with and without Cu **B** – 60,80 kV with Cu **C –** 60 kV with increased mA

Fig 48: X-ray tube evolution

a) c 1980 – Primarily radiative cooling Source- Siemens Healthineers

b) c 1990 Conduction cooling via liquid metal bearings and external heat exchanger Source- Philips Healthcare

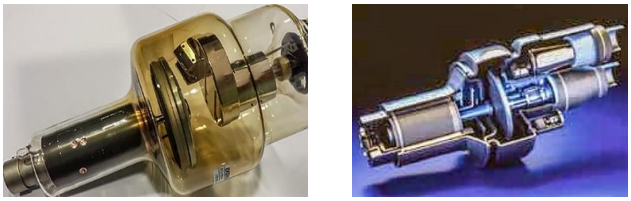

X. DIGITAL IMAGE PROCESSING (1980-2010)

Electronic processing of clinical radiographic and fluoroscopic images began in the late 1970's. Capp's 1980 New Horizons lecture at the RSNA[44] provides a snapshot of this watershed (Fig 49). The transition from analog to digital video was much earlier than Capp's forecast. It was driven by increasing availability of small computers capable of image processing at video speeds (e.g. 30 fps) and the replacement of analog video-tubes with CCD cameras. Two major results were real-time processing of fluoroscopic imaging streams and Digital Subtraction Angiography (DSA)

Managing the characteristics of analog video images was challenging. In this era, temporal noise averaging was physically achieved by selecting video pickup tubes and display monitors with appropriate characteristics. All processing affected the entire image. Overall temporal resolution was determined by the video-framerate, a value usually linked to the local power-line frequency for broadcast compatibility and synchronization. As discussed above, greater temporal integration reduced the appearance of quantum noise at the expense of increased motion blur. Image brightness and contrast could be electronically adjusted. Spatial resolution was strongly influenced by the scan pattern and number of available scan lines. None of these factors could be easily changed to either enhance imaging appearance in real time (e.g. automatic contrast adjustments) or optimize imaging to meet differing requirements of different procedures.

Fig 49: 1980 forecast of electronic image handling in 2000

In this view, image capture and image processing are in the analog domain. Image storage is digital. Film has disappeared.

Source – Capp[44] – permission pending

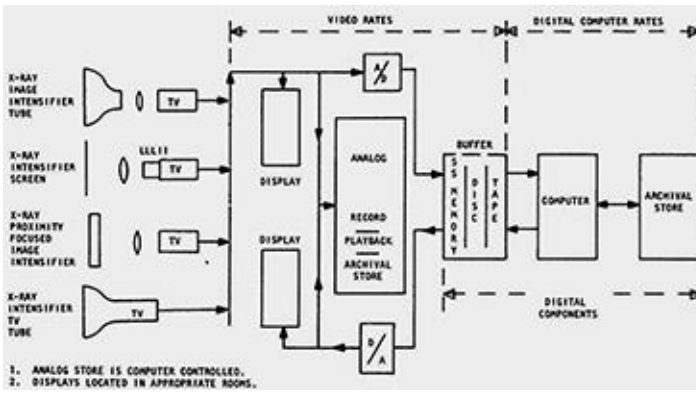

XI. DIGITAL SUBTRACTION ANGIOGRAPHY (DSA) – (1980-2019)

Photographic subtraction was used in the mechanical film-changer era to document blood flow. An image obtained before contrast-media reached the region of interest is selected as the mask. A negative version of this image is produced in the darkroom. The single negative mask was then physically registered with subsequent images to produce the subtracted image.

Unsharp masking involved placing a spacing sheet of glass between the mask and a later image. Mask blur is determined by the thickness of the spacer. This tedious procedure was seldom used to subtract more than a few of the images acquired during a study. Electronic subtraction in real-time or near-real-time was developed and deployed as soon as the enabling analog and technologies permitted [45-48]. Fig 50 provides system schematics of subtraction radiography and subtraction fluoroscopy. Much of the work is performed in the analog domain because the technology of this time did not support fully digital equipment. Figure 51 illustrates some of the hardware used for two early digital subtraction systems. The subtracted images were in video format and either recorded as video or photographed from a CRT display. Maintaining image quality for fluoroscopes that use image intensifiers and perform analog image processing is difficult because of instabilities and image noise added by these elements. The introduction of fully digital image processors enabled useful functions such as better registration of live and mask images, and road-mapping (partial subtraction that provided enough anatomical reference to facilitate device movement). DSA, including its sub modes, rapidly became, and remains, a cornerstone of FGI.

Fig 50: 1980 Hybrid Subtraction Angiography

See text

Source - Ergun[45] – permission pending

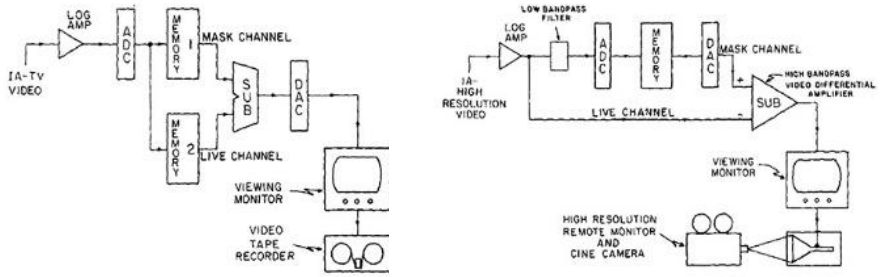

Fig 51: 1980 DSA Hardware

a) Note the size of the electronics cabinet needed to house the early `image processor. Source – Siemens Healthineers

b) Controls used for a first-generation clinical DSA system. The image processor for this device also filled a full-size electronics cabinet.

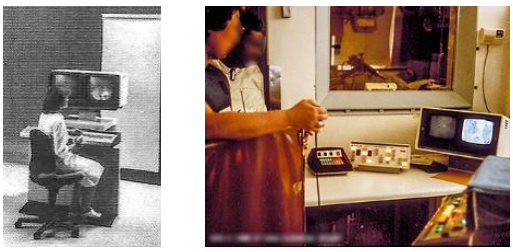

Subtraction angiography (e.g. DSA) removes fixed information found in both the mask and live image from the resultant. All X-ray images contain stochastic quantum noise with the point-to-point noise intensity proportional to the square root of the local signal intensity. Other noise sources may be present with different spatial distributions. Random noise does not subtract but adds and produces more noise in the difference image than in either initial image. The final step in DSA is to greatly increase the contrast of the display to improve visibility of blood vessels or other moving structures. This also increases the visibility of image noise. The target-to-noise ratio can only be increased by increasing radiation dose. Thus, DSA requires about an order of more radiation per frame than unsubtracted imaging of the same object. Unnecessary irradiation is minimized if X-ray quantum noise is the dominant noise source in an image. This can be evaluated if the noise in the subtracted image differs from place to place (e.g. near and far from subtracted bone). This appearance is called a noise-print[49] and can serve as a quick quality test using clinical DSA images.

DSA using CO_2 as the contrast agent (available since the 1980's) can be of clinical benefit. Images are recorded while a CO_2 gas injection displaces blood. The optimum technique uses a higher KvP to reduce unwanted photoelectric attenuation in the patient's tissues, and image stitching to produce a composite image or image series of the entire artery by following the CO_2 bubble through the patient's arteries over time.

XII. IMAGE PROCESSING, DISPLAY, AND STORAGE (1990 – 2010)

Digital video eliminates many of the constraints inherent in powerline synchronized analog video. Working back from the display toward the imaging hardware: Displays are not constrained by the imager's pixel size or acquisition frame rate. Images are interpolated and scaled to transform the acquisition version into the matrix size used for display. These images are refreshed in the display at a rate well above the eye's critical flicker frequency. In its simplest form, the same data is shown multiple times until replaced by a new image. In addition to decoupling acquisition and display rates, this provides the functionality for pulsed fluoroscopy and acquisition (X-ray production during a fraction of the available frame time).

Frames can also be combined in an arbitrary manner. DSA image processing is inherent, including technologies that were impossible with analog video such as frame by frame pixel shifts to compensate for unwanted anatomical motion during a run. Noise reduction is obtained by recursive filtering: A fraction of the previous image is added to the newly acquired data.

Noise reduction increases as the number of previous acquisitions contribute. The downside is that the remnants of the older images produce ghosts and blur of moving objects. This effect is programmable and can be configured at tableside to match the immediate clinical imaging requirement. Compare this with achieving this balance by changing video-tube technologies in the analog era.

Images can be visually sharpened using a variety of processes such as unsharp masking. This technique combines sharp and blurred versions of the same image. A similar process occurs in the retina by interactions at a neural level. The results of the process can be seen as Mach bands outlining the edges of recorded or visualized objects. Here again, the magnitude of the effect in the digital domain can be configured at tableside.

The relationship between the X-ray intensity illuminating a detector pixel and the brightness of that pixel on a display is defined by an arbitrary look-up-table. A simple example is the window-level controls found on CT scanners as well as fluoroscopes. Different look-up-tables are applied to different imaging tasks, and each table can be immediately tuned as needed.

Viewing monitors are a non-trivial link in the fluoroscopic imaging chain. Monitors used for primary radiographic and mammographic diagnosis are available with built-in quality control tools. Current fluoroscopic systems often include an injected or stored digital SMPTE test pattern[50]. Objects are provided to assess spatial-resolution, gray-scale performance, as well as system generated artifacts. Figure 52 illustrates this test including examples of white and black clipping. Fluoroscopic monitors are expected to simultaneously show both the 5% block (in the 0% black block) and the 95% block (in the 100% white block) when viewed under clinical working laboratory light levels.

Fig 52: SMPTE Test Pattern
a) Black clipping
b) Full range – Expected with normal room light.
c) White clipping

Original Source - ANON

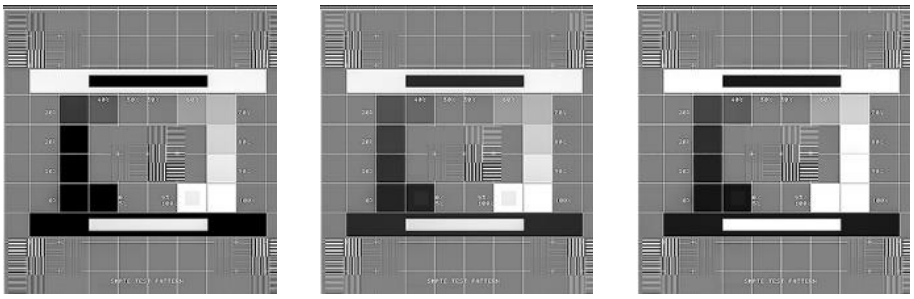

A **B** **C**

As described by Morgan in 1966 [20], the ability to perceive an object includes the effects such as the angle subtended by the object on the observer's retina. Increasing the angular size of an object by any means (e.g. using magnification mode in an image intensifier, digitally magnifying an image, or simply using a larger monitor) may affect its perceptibility. In some cases, reacting to larger images can improve operator radiation protection. Some interventional fluoroscopists using conventional (19") monitors tend to lean over the patients during imaging to better see small arteries. The same operators often stand erect when performing the same cases using large (60") monitors. They seem to be adjusting their posture to best see the target vessels. The posture change reduces their irradiation simply because it moves them away from the patient's scatter field.

Fig 53: Effect of monitor size on operator posture.
a) 19": The operator is leaning over the patient to better see the arteries during a cine run.

b) 60": The magnified image permits the operator to stand away from the patient.

Digital medical images are among the largest files (both individually and in total) in healthcare. In the context of this review, digital images can be stored within the fluoroscope or in an external archive such as a PACS. Image transport is via networks or media. The deployment of digital images was, and continues to be, facilitated by the evolving DICOM standard. A review of this area is beyond the space limitations of this paper.

Figure 54 provides a glimpse back into the transition era. These images were taken in the interventional cardiology laboratory of Lenox Hill Hospital in New York City. Cine media included film, analog videotape, and several digital CD formats.

Fig 54: c 2000 Transition from analog to digital image management

a) Cine film processor and darkroom.

b) Cine film viewer. The boxes in the background are part of the daily image transfer between the lab and its off-site archive. Each box contains 50 rolls of cinefilm. Image storage and retrieval was on a 24-hour cycle.

c) One day's cases for one physician. Images are on film, CD, and analog videotape.

Source for all - Balter – Lenox Hill Hospital, New York

XIII. EXAMINATION CONFIGURATION

Fluoroscopic procedures usually include the operator's direct adjustments of imaging parameters and often substantial a-priori information about the specific patient's medical condition. Almost all the fluoroscopes manufactured after the 1970s provide a selection of pre-configured examination and patient specific technical sets. Many of the pre-configured X-ray production and image processing factors can be overridden by operators to suit their immediate imaging needs while a procedure is in progress. At present, high-end fluoroscopes may be set to any of several thousand distinct configurations. Each configuration potentially differs from the others in its radiation management behavior, its image processing characteristics, and usually in both domains.

XIV. SOLID-STATE FLUOROSCOPIC IMAGE RECEPTORS (2000-2019)

The image intensifier tubes themselves began to be replaced by solid-state detectors starting c 2000 [51-56]. Solid state detectors (flat panels or FP) were commercially available in 2000. Both indirect (X-ray to light to electronic signal) and direct (X-ray directly to electronic signal) technologies were known. (Figure 55)

Fig 55: Indirect and Direct Flat Panel Detectors

Schematic sketch of information carriers

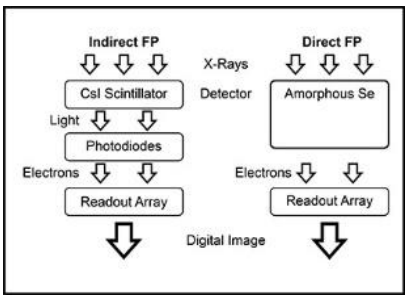

The same CsI scintillator is used in late-model image intensifiers and indirect FPS. Input dose rates for fluoroscopy and fluorography are similar in both domains. However electronic noise levels are somewhat higher in a FPS and amplified with digital magnification. This does not occur in an II using electro-optical zoom. Thus, fluoroscopic dose rates are usually to be a bit higher in FPS compared to late-model image intensifiers. Dose rates needed to meet the imaging requirements of fluorography are sufficiently high that they are independent of technology. Radiation savings attributable to FPS are due to better radiation management in newer designs[57].

The need for video frame rates (e.g. 30 fps) resulted in the use of indirect technology for the first generation of FP detectors. This technology continues to be found in most FP detectors produced in 2019. The radiation detection element that is continuous sheet of CsI, essentially identical to the CsI element in the image intensifier of the era. The detector's nominal physical size was 20 x 20 cm. Light from the CsI was detected by an array of 1000 x 1000 photodiodes/amplifiers. The nominal pixel size of this device was a bit under 0.2 x 0.2 mm. Space is needed in the photodiode array for amplifiers and readout electronics. Thus, the active surface of a single photodiode only filled about 70% of the nominal pixel size. X-ray photons interacting in other areas contributed to the signal due to light diffusion in the CsI layer. Figure 56 illustrates hardware elements of indirect FP detectors

Fig 56: Indirect Flat Panel

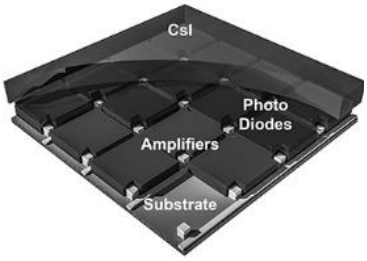

Detector elements

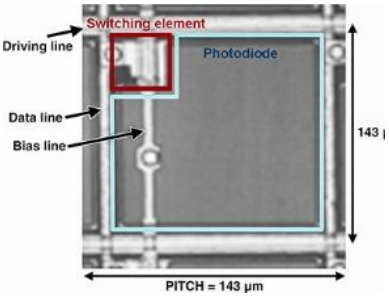

Pixel – Source - Philips Healthcare

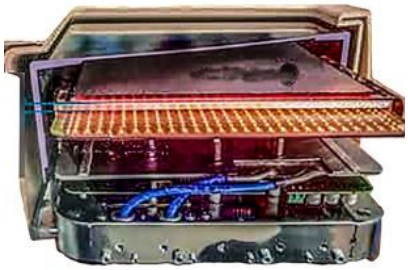

Assembly with electronics and thermal regulators. – Source - Philips Healthcare

FPs reduce or eliminate several inherent image-intensifier artifacts. These include vingetting (images dimmer in the periphery relative to the center), pincushion-distortion (result of projecting a curved input screen onto a flat output screen). S-distortion (electro-magnetic field influence on the II's electron optics), and II dynamic range limitations.

Three separate actions occur when the field of view of a flat-panel system is changed: 1) Irradiation is limited to a subset of the pixels in the detector. 2) Detector pixels may be binned to comply with bandwidth limitations of the detector's output channel, and 3) The output image is scaled by an external image processor to fit the properties of the image display. The spatial resolution of a FP varies with magnification mode in a fundamentally different way than for an image intensifier. In an II, the limiting resolution element is the output screen or video camera. Changing the FOV in an II projects a larger or smaller portion of the input screen onto the fixed size output system. In the II, resolution increases inversely with the diameter of the input FOV. However, in a FP, a greater or lesser number of fixed size pixels are irradiated when the FOV is changed. The inherent resolution of the detector elements is unaffected by changes in FOV.

Spatial resolution of a FP system is affected by two additional factors: In large format FPs, the total number of pixels exceeds the fluoroscope's image matrix size. Pixels are binned in the detector electronics to reduce the output matrix for large FOVs. (typically, 2 x 2 into 1 x 1). Binning is removed when the FOV is small enough to fit the output matrix. The resultant spatial resolution has a step increase at the FOV where binning is no longer applied. A second, less common, use of binning is to accommodate very fast video frame rates (e.g. 60 fps) within the bandwidth of the fluoroscope's electronics. When this occurs a step in spatial resolution is expected when the frame rate is reduced.

Because noise perceptibility is increased with increasing magnification projected onto the observer's eye, it is necessary to increase radiation dose as magnification is increased. Essentially, visual noise limitation requires that the same number of photons are used to form a pixel irrespective of its size. As discussed above, image intensifier systems require an increase in radiation dose rate proportional to the ratio of the square of the FOV with image-intensifier magnification to account for the physical loss of minification gain when a smaller FOV is selected. Ignoring any bundling-unbundling transition, changing the zoom on a FPS with a corresponding secondary magnification by the system's image processor is usually accompanied by a deliberately programmed increase in patient dose rate. It was empirically found that increasing fluoroscopic dose rate inversely proportional to the linear size of the active FOV produced satisfactory clinical results for both fluoroscopy and acquisition modes.

XV. DIGITAL IMAGE PROCESSING (2010-2019)

Fluoroscopic X-Ray tubes and image receptors have not changed in any fundamental manner in the past decade. Increased image processing power has had a substantial impact on both clinical conspicuity and radiation use in the same time interval.

The job of the image acquisition elements of the fluoroscopic system is to deliver technically adequate images to the system's digital image processor. These images are then processed, and the results delivered to the observer. In modern terminology, these image stages are called 'for processing' and 'for presentation'. As discussed below, presentation images usually undergo non-linear transformations, that are configured based on presumed clinical content. Many fluoroscopes delivered after 2010 have enough computational resources to provide different algorithms in different regions of the same image. These algorithms rely on a-priori knowledge of the examination in progress. Such information is currently supplied by the operator's selection of an examination-set. A future fluoroscope might improve selections by analysis of the patient's current and historical images.

Figure 76 sketches information flow in 1966 and 2016 fluoroscopes. In both eras, X-rays interact with a patient to produce a modulated beam which is then detected and converted into a visible image projected into the observer's eye-brain system. The characteristics of the 1966 image were fixed by a combination of imaging hardware and operating conditions (e.g. kVp, mAs). In 2016, the X-ray source has additional controls that affect images (e.g. variable framerate, and shaped X-ray

spectrum). Also, controllable image processors and displays are in the information flow line between the imaging system and the observer.

Fig 57: Fluoroscopic Information Flow

a) Morgan (1966) – permission pending

b) based on Lendil (2018)

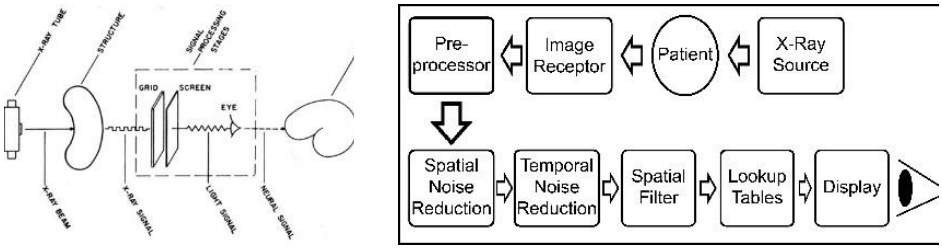

Global temporal averaging is an inherent characteristic of analog video tubes. As discussed above, changing tube types altered both noise characteristics and motion blur. The lack of lag in newer camera types increased the appearance of noise, including X-ray quantum noise. Image processors can supply temporal averaging using the recursive filtering algorithm. Figure 58 illustrates the effects of adding recursive filtering. The original images were acquired using pulsed fluoroscopy with short pulses. There is minimum motion blur of the rapidly moving guidewire in the original images (it is in a different position in each image). The number of older images contributing to the current image increases with increased recursion. This results in ghosting of previous guidewire positions (arrow).

Fig 58: Global Temporal Recursive Filtering

a) No recursion

b) Low recursion

c) High recursion

Visual noise decreases and ghosts of moving objects increase with increased recursion

Source- Siemens Healthineers - Lendil

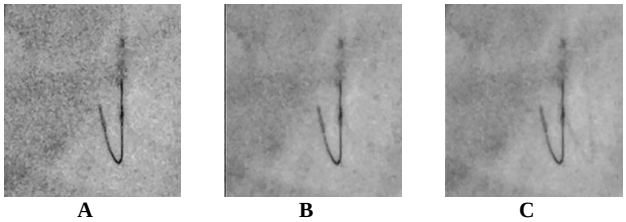

Many algorithms can be used to modify the global appearance of the images for the purpose of increasing the perceptibility of clinically important information. Four of these are sketched in Figure 59.

Fig 59: Image processing algorithm components

a) Single frame smoothing

In this example, a simple gaussian blur has been used to process the right-hand image shown in Fig 58

b) Temporal (Multi frame) smoothing discussed in text above

c) Automatic motion compensation

d) Multi-parameter image enhancement

b-d) Source – Philips Healthcare - Jans

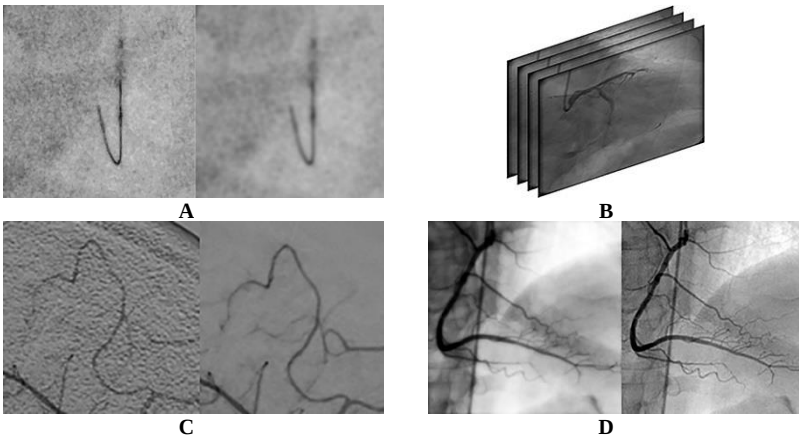

Image processors are now fast enough to apply different algorithms in different parts of the same image, and in different but corresponding parts of an image sequence. Figure 60 illustrates single-frame local processing. The image processor has identified the small contrast filled artery in the image on the left. On the right, the original pixel data is unchanged near the vessel and pixel averaging is applied to smooth the background appearance.

Fig 60: 2018 Single Frame Local processing

a,b) Clinical Image. Less spatial averaging is applied near the artery. Source: Philips Healthcare - Jans

c) Last-image-hold of a portion of a daily fluoroscopic QA phantom. Less spatial averaging

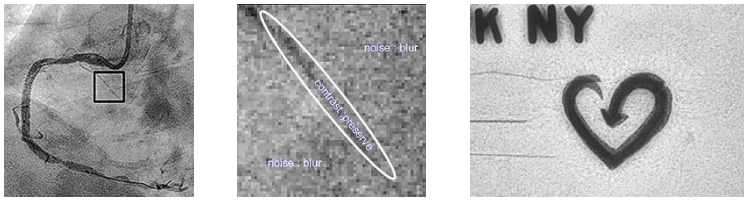

near lead markers and guide wires, more in uniform areas of the image. Source – Columbia

A **B** **C**

Figure 61 is a photographic simulation of multi-frame local processing. The local focus in this simulation is a vertical section of the right coronary artery. Noise was separately added to three replicas of the same initial image before combining them.`

Fig 61: Multi- Frame (temporal) Local Processing Simulation

a) Single image

b) Three replicas summed without motion

c) Replicas summed with simulated motion.

d) Replicas summed except for the region near the vertical RCA segment, single image data used here.

Note the ghosting in summed areas in c and d; note the increased noise near the RCA in d

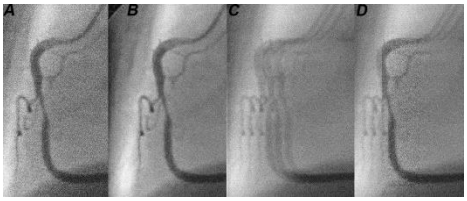

The importance of prior and real-time control of fluoroscopic image processing will continue to grow. The operator is a key node in managing automatic image analysis and processing as well as in other aspects of controlling and optimizing the settings and use of the entire fluoroscopic system. (Fig.62). The starting point is the pre-procedure transfer of patient current and historical data, procedural intent, operator preference, and other factors.

Conditions can and will change during a procedure. The goal is to continuously optimize both image acquisition and image processing parameters when these changes occur. Some (e.g. substituting CO_2 for Iodine as a contrast medium) should be detectable by automatic image analysis. Others (e.g. replacing a steel angiographic guidewire with a Platinum plated version) may not be recognizable by the image processor. The challenge is to maintain optimization without unnecessarily distracting operators and their assistants from essential patient care.

Fig 62: A-priori, automated, and operator- controlled image processing

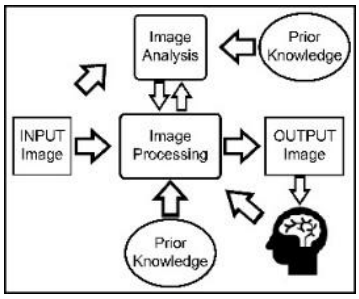

a) Image processing and analysis uses both prior knowledge and feedback from the observer – Based on Lendil 2018

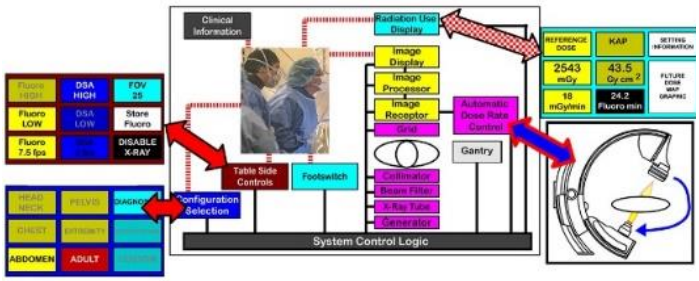

b) The operator is a key node in many fluoro control loops.

XVI. COMMENT

Radiologic imaging procedures needed to achieve a clinical goal should be performed in a manner that optimizes the balance between potential clinical benefits and all risks (not just minimize radiation)[58]. Fluoroscopic optimization differs from most other modalities in that achieving patient benefits imposes risks on both patients and staff.

Information flow can broadly be segmented into acquisition, processing, display, and utilization (Figure 63). Each of these domains should be optimized by itself and with consideration of the other domains. Equipment quality testing has traditionally focused on acquisition. The availability of 'for-processing' images between the acquisition and processing domains provides the opportunity to develop better testing tools for the imaging hardware and its configuration. Potentially, a digital test image (SMPTE is one simple example) could be inserted into the image processor and separately test the processing-display portion of the system. Metrics describing the operators' use of the fluoroscope and the clinical result of such use are under development[58]. Image quality evaluations might eventually include short-term and long-term clinical outcomes from large numbers of procedures.

Fig 63. Information Flow

The for-processing, for-display, and clinical-utilization nodes could be used for quality evaluations.

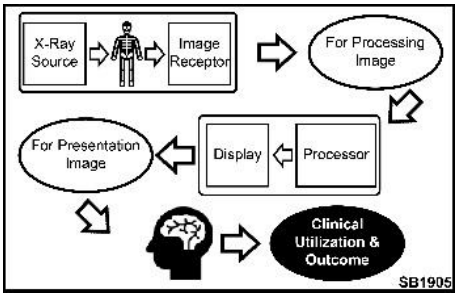

Fluoroscopic technology has progressed over the past 125 years. In the first decade, the operator needed a considerable body of physical and technical knowledge in order to adjust the system to for it to work at all. In the most recent decade, the operator's main challenge is to supply the system with necessary and sufficient information so that a well configured fluoroscope can self-optimize to meet immediate clinical needs. A consequence of this requirement is that equipment designers, service personnel, applications specialists, and medical physicists must be aware of the specific imaging requirements needed to meet different clinical needs. Achieving and maintaining an appropriate level of clinical understanding is one of the major tasks for continuously improving imaging in the 21st century.

XVII. REFERENCES

1. W. C. Roentgen, Aus den Sitzungsberichten der Würzburger Physik.-medic. Gesellschaft Würzburg, 137-147 (1895).
2. W. C. Roentgen, Aus den Sitzungsberichten der Würzburger Physik.-medic. Gesellschaft Würzburg, , 11-17 (1896).
3. W. C. Roentgen, Mathematische und Naturwissenschaftliche Mitteilungen aus den Sitzungsberichten der Königlich Preußischen Akademie der Wissenschaften zu Berlin, 392-406 (1897).
4. ANON, Nature 54 (1388), 109-112 (1896).
5. S.J.R., Nature 54 (1409), 621-621 (1896).
6. ANON, Scientific American (April 4, 1896), 219 (1896).
7. G. King, (smithsonian.com, 2012), Vol. 2019.
8. ANON, Scientific American (August 8, 1897), 88-89 (1897).
9. T. C. Gilcrist, Bull Johns Hopkins Hosp 8 (71) (1897).
10. S. Tousey, MEDICAL ELECTRICITY AND RONTGEN RAYS WITH CHAPTERS ON PHOTOTHERAPY AND RADIUM, first ed. (W. B. SAUNDERS COMPANY, PHILADELPHIA, 1910).
11. I. Rock, An Introduction to Perception. (Macmillin Publishing Company, New York, 1975).
12. B. A. Wandell, Foundations of Vision. (Sinauer Associates Inc, Sunderland, MA, 1995).
13. W. E. Chamberlain, Radiology 38 (4), 383 - 413 (1942).
14. F. J. Hodges, Radiology 38 (4), 453-461 (1942).
15. R. E. Sturm and R. H. Morgan, American Journal of Radiology 62 (1949).
16. A. Rose, J Opt Soc Am 38 (2), 196-208 (1948).
17. J. W. Coltman, Radiology 51 (3), 359-367 (1948).
18. NBS, 1963.
19. T. Holm and R. D. Moseley, Jr., Radiology 82 (5), 898-904 (1964).
20. R. H. Morgan, Radiology 86 (3), 403-416 (1966).
21. N. R. Silverman, Radiology 103 (2), 263-265 (1972).
22. B. M. Lantz, J. M. Foerster, D. P. Link and J. W. Holcroft, AJR Am J Roentgenol 134 (6), 1161-1168 (1980).
23. D. M. Hynes, E. W. Edmonds, K. R. Krametz and D. Baranoski, Radiology 133 (3 Pt 1), 751-755 (1979).
24. S. Balter, F. M. Sones, Jr. and R. Brancato, Circulation 58 (5), 925-932 (1978).
25. E. W. Gertz, J. A. Wisneski, R. G. Gould and J. R. Akin, Am J Cardiol 50 (6), 1283-1286 (1982).
26. H. Dash and D. M. Leaman, J Am Coll Cardiol 4 (4), 725-728 (1984).
27. M. R. Pitney, R. M. Allan, R. W. Giles, D. McLean, M. McCredie, T. Randell and W. F. Walsh, J Am Coll Cardiol 24 (7), 1660-1663 (1994).
28. L. E. Watson, M. W. Riggs and P. D. Bourland, Health Phys 73 (4), 690-693 (1997).
29. S. Balter, Radiat Prot Dosimetry 94 (1-2), 183-188 (2001).
30. E. Kuon, M. Schmitt and J. B. Dahm, Am J Cardiol 89 (1), 44-49 (2002).
31. E. Kuon, M. Gunther, O. Gefeller and J. B. Dahm, Rofo 175 (11), 1545-1550 (2003).
32. A. Komemushi, N. Tanigawa, S. Kariya, H. Kojima, Y. Shomura and S. Sawada, J Vasc Interv Radiol 16 (10), 1327-1332 (2005).
33. N. T. Fitousi, E. P. Efstathopoulos, H. B. Delis, S. Kottou, A. D. Kelekis and G. S. Panayiotakis, Spine (Phila Pa 1976) 31 (23), E884-889; discussioin E890 (2006).
34. B. A. Schueler, T. J. Vrieze, H. Bjarnason and A. W. Stanson, Radiographics 26 (5), 1533-1541; discussion 1541 (2006).
35. O. Dragusin, R. Weerasooriya, P. Jais, M. Hocini, J. Ector, Y. Takahashi, M. Haissaguerre, H. Bosmans and H. Heidbuchel, Eur Heart J 28 (2), 183-189 (2007).
36. K. P. Kim and D. L. Miller, Radiat Prot Dosimetry 133 (4), 227-233 (2009).
37. L. W. Klein, D. L. Miller, S. Balter, W. Laskey, D. Haines, A. Norbash, M. A. Mauro and J. A. Goldstein, Radiology 250 (2), 538-544 (2009).
38. B. A. Schueler, Tech Vasc Interv Radiol 13 (3), 167-171 (2010).
39. O. P. Haqqani, P. K. Agarwal, N. M. Halin and M. D. Iafrati, J Vasc Surg 55 (3), 799-805 (2012).
40. D. L. Miller, Health Phys 105 (5), 435-444 (2013).
41. G. Christopoulos, A. C. Papayannis, M. Alomar, A. Kotsia, T. T. Michael, B. V. Rangan, M. Roesle, D. Shorrock, L. Makke, R. Layne, R. Grabarkewitz, D. Haagen, S. Maragkoudakis, A. Mohammad, K. Sarode, D. J. Cipher, C. E. Chambers, S. Banerjee and E. S. Brilakis, Circ Cardiovasc Interv 7 (6), 744-750 (2014).

42. A. den Boer, P. J. de Feyter, W. A. Hummel, D. Keane and J. R. Roelandt, Circulation 89 (6), 2710-2714 (1994).
43. R. M. Gagne, P. W. Quinn and R. J. Jennings, Med Phys 21 (1), 107-121 (1994).
44. M. P. Capp, Radiology 138 (3), 541-550 (1981).
45. D. L. Ergun, C. A. Mistretta, R. A. Kruger, S. J. Riederer, C. G. Shaw and D. P. Carbone, Radiology 132 (3), 739-742 (1979).
46. R. A. Kruger, C. A. Mistretta, T. L. Houk, W. Kubal, S. J. Riederer, D. L. Ergun, C. G. Shaw, J. C. Lancaster and G. G. Rowe, Invest Radiol 14 (4), 279-287 (1979).
47. A. B. Crummy, C. M. Strother, J. F. Sackett, D. L. Ergun, C. G. Shaw, R. A. Kruger, C. A. Mistretta, W. D. Turnipseed, R. P. Lieberman, P. D. Myerowitz and F. F. Ruzicka, AJR Am J Roentgenol 135 (6), 1131-1140 (1980).
48. C. G. Shaw, D. L. Ergun, R. A. Kruger, C. A. Mistretta, A. B. Crummy, D. Myerowitz, C. M. Strother, J. Sackett, M. Van Lysel, W. Zarnstorff and W. Turnipseed, Nuclear Science, IEEE Transactions on 27 (3), 1042-1046 (1980).
49. S. Balter, D. Ergun, E. Tscholl, F. Buchmann and L. Verhoeven, Radiology 152, 195-198 (1984).
50. D. S. Groth, S. N. Bernatz, K. A. Fetterly and N. J. Hangiandreou, Radiographics 21 (3), 719-732 (2001).
51. G. Pang, W. Zhao and J. A. Rowlands, Med Phys 25 (9), 1636-1646 (1998).
52. J. H. Siewerdsen, L. E. Antonuk, Y. el-Mohri, J. Yorkston, W. Huang and I. A. Cunningham, Med Phys 25 (5), 614-628 (1998).
53. M. Strotzer, J. Gmeinwieser, M. Volk, R. Frund, J. Seitz, C. Manke, H. Albrich and S. Feuerbach, AJR Am J Roentgenol 171 (1), 23-27 (1998).
54. M. Strotzer, M. Volk and S. Feuerbach, Electromedica 66 (2), 52-57 (1998).
55. H. D. Kubo, E. G. Shapiro and E. J. Seppi, Med Phys 26 (11), 2410-2414 (1999).
56. N. Matsuura, W. Zhao, Z. Huang and J. A. Rowlands, Med Phys 26 (5), 672-681 (1999).
57. S. Balter, Catheter Cardiovasc Interv 63 (3), 331 (2004).
58. S. Balter, M. Brinkman, S. Kalra, T. Nazif, M. Parikh, A. J. Kirtane, J. Moses, M. Leon, A. Feri, P. Green, Z. A. Ali, M. Liao and D. Karmpaliotis, EuroIntervention 13 (12), e1468-e1474 (2017).

XIX. AUTHOR INFORMATION

Stephen Balter is a Professor of Clinical Radiology (physics) and Medicine at Columbia University.

He is an international authority on all aspects of medical fluoroscopy.

Dr. Balter is a member of Council of the National Council on Radiation Protection and Measurements. He served as the chair of NCRP Report-168 – Radiation Dose Management for Fluoroscopically-Guided Interventional Medical Procedures.

Email: sb2455@cumc.columbia.edu